alvikite with some carbonatitic breccia, sövite and ferro-carbonatite. Ferrocarbonatite is mostly distributed in the peripheral zone of the complex as ring-dykes.

South Ruri Hill is a cylindrical massive cabonatite complex (diameter=2.5 km), which is the largest single carbonatitic body in the Homa Bay area. This comprises alvikite, sövite, carbonatitic breccia, and ferrocarbonatite. Ferrocarbonatites occur as dykes in the peripheral zones of the complex.

The geological plan and profiles of the area are presented in Fig. II–1–1.

1–3 Results of Geological Survey

Generalized geological columner sections are presented in Fig. II–1–2.

1–3–1 North Ruri Hill North Sector

This sector is situated in the northern slope of North Ruri Hill Carbonatite complex (Fig. II–1–1, II–1–6).

The geology of the sector comprises the basement Nyanzian Metabasalt and carbonatitic rocks composed of alvikite and ferrocarbonatite which have intruded the basement.

The geological plan and profiles of the sector are presented in Fig. II–1–3.

(1) Nyanzian Metabasalt

The unit is distributed in the piedmonts of the North Ruri Hill. The rocks are dark grey to dark greenish grey, fine-grained compact volcanics. Calcite veinlets occur in the rocks resulting in yellowish grey in colour.

(2) Alvikite

The unit is distributed almost all areas of the sector forming clifs of several tens of meters in height in the south half of the sector.

The rocks are pale grey, fine to medium grained, in some places coarse grained and have banded structures. The major constituent minerals are carbonates with minor mica, magnetite and apatite.

(3) Alvikite breccia

The unit is distributed in the southeast corner and south part of the sector in small scales.

The rocks are composed of angular to subrounded breccias of alvikite, sövite and metabasalt, and reddish brown fine matrix. Contamination by ferric–oxide are remakable throughout the rocks. The amount of breccias is very variable.

(4) Ferrocarbonatite breccia

The unit is distributed in the middle of the north half of the sector in an area of about

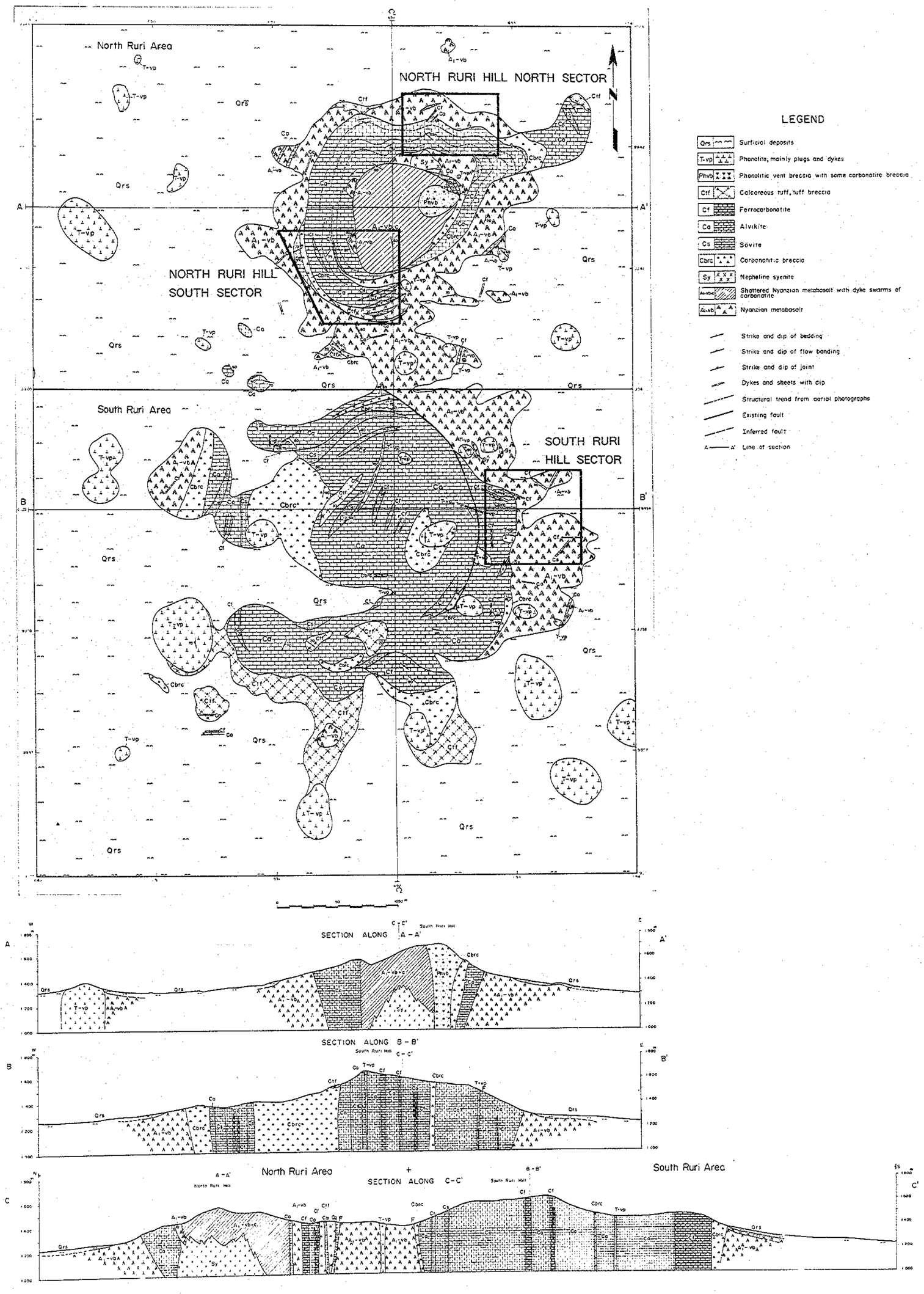

Fig. II – 1 – 1 Geological Map of the North & South Ruri Hill Area (Phase I Results)

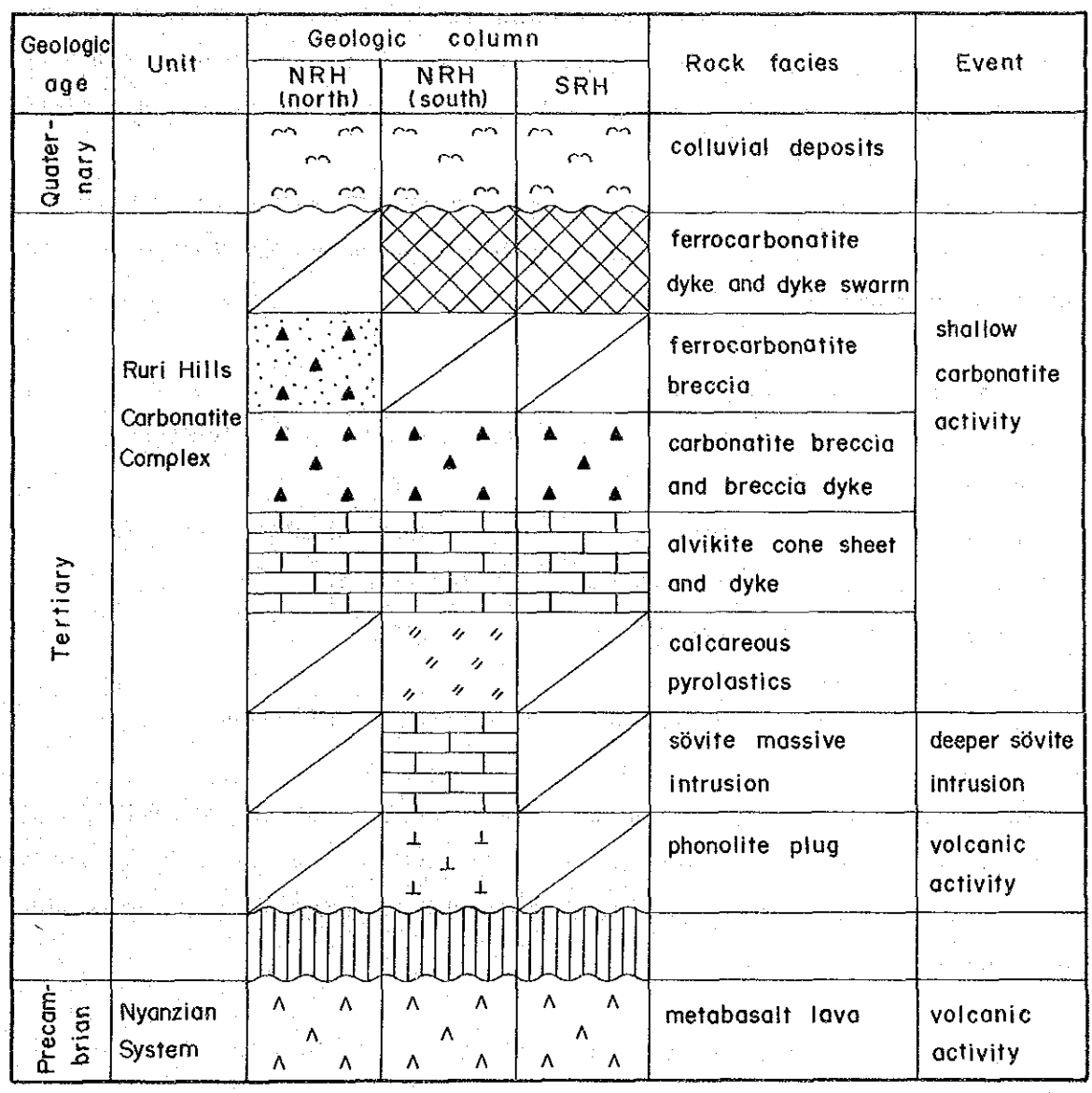

Fig. II – 1 – 2 Generalized Geological Columnar Section of the North & South Ruri Hill

300x100 m trending in E–W direction. The location is just northern marginal part of North Ruri Hill Carbonatite Complex and the rocks contact with Nyanzian Metabasalt.

The rocks shows variable colours such as brown, dark brown and reddish brown, and the variation in colour is mainly caused by oxidation of iron bearing minerals. The rocks are heterogeneous both in amount and size of breccias, and shows banded structure in some place where the amount of breccias is very small.

The rocks have been intruded by small dykes and network veinlets of brown to black ferrocarbonatites which are estimated to be the products of the latest stage of intrusion of the North Ruri Hill Carbonatite Complex.

1–3–2 North Ruri Hill South Sector

This sector is situated in the west to south slope of the South Ruri Hill (Fig. II–1–1, II–1–6).

The geology of the sector comprises the basement Nyanzian Metabasalts, calcareous pyroclastic rock, alvikite, sövite, ferrocarbonatite and carbonatite breccias.

The geological plan and profiles are presented in Fig. II–1–4.

(1) Nyanzian Metabasalt

The unit is distributed in the west and south of the sector, and in the northeast of the sector intruded by dyke swarms of carbonatite.

The rocks are dark grey to dark greenish grey, fine-grained and compact. In the marginal parts with the carbonatite complex particularly in the southern marginal part, the rocks show pale brown in colour and have undergone brecciation, resulting to change gradually to carbonatite breccia on the north of the unit.

(2) Alvikite

The unit is distributed in the central part of the sector as a central massive body and in the periphery of the body as ring dykes or sheets.

The rocks shows variable colour such as pale grey, grey, greyish brown and dark grey.

The rocks are fine to medium-grained and banded, and comprise carbonate minerals with accessary mica, pyroxene, magnetite and apatite.

(3) Sövite

The unit is distributed in the central part of the north half of the sector being enclosed by the central alvikite massive body. The boundary between the alvikite body and the unit is gradual, and the unit have many xenolith-like bodies of metabasalt.

The rocks are pale grey to white, massive, coarse-grained and comprise carbonate minerals with accessary biotite, pyroxene, magnetite and large biotite crystals (1 cm in diameter) in some places.

(4) Ferrocarbonatite

The unit is distributed as a group of small dykes (dyke swarms, Fig. II–1–7) in the south part of the sector and as dykes in the west and southwest of the sector.

The sizes of dykes are several centimeters to 1 m in width and several meters to several tens of meters in length in the dyke swarm zone and several to twenty meters in width and 250 m in maximum length in the west and southwest of the sector.

The rocks shows dark grey, dark brownish grey, dark brown and pale brown in colour. The facies are very variable in texture and, mineral composition. Some shows banded structure and brecciated structure. Some includes a lot of magnetites.

The rocks comprises mainly carbonate minerals and goetites after iron oxide minerals.

(5) Carbonatitic breccia

The unit is distributed as dykes which have intruded into metabasalt in the west of the sector.

The unit is thought to be intrusive breccia facies or xenolith-rich facies of alvikites.

The rocks comprise breccias of alvikite and metabasalt, and alvikitic matrix. The rocks change gradually both to alvikite and metabasalt.

(6) Calcareous pyroclastics

The unit is locally distributed in the south part of the sector.

The unit comprises pale grey calcareous lapilli tuff, calcareous tuff and intercalating pale grey calcareous mustone.

The rocks comprises lapillis of metabasalts, alkaline intrusives and volcanic rocks, and calcareous ash rich in magnetite and biotite.

The rock have been intruded by alvikites and ferrocarbonatites, showing that they are earlier products in Ruri Hill carbonatite activity than the main rock facies of the North Ruri Complex.

1–3–3 South Ruri Hill Sector

This sector is situated in the east slope of the South Ruri Hill (Fig. II–1–1, II–1–6).

The geology of the sector comprises basement Nyanzian Metabasalt, alvikite, ferrocarbonatite, carbonatitic breccia and phonolite.

The geological plan and profiles are presented in Fig. II–1–5.

(1) Nyanzian Metabasalt

The unit is widely distributed in the sector except west part of the sector.

The rocks have undergone shattering by the intrusion of carbonatite, resulting in fragmental or breccia-like occurrences.

The rocks are dark grey to dark greenish grey, fine-grained, non porphyritic and compact. Megascopically the rocks have been stained by ferric iron oxide and filled by calcite along fractures.

(2) Alvikite

The rocks are distributed in the west part of the sector as a part of margin of Ruri Hill Carbonatite Complex and in the midde to east of the sector as small dykes.

The rocks are grey, greyish brown and brown in colour, and fine to medium-grained. Megascopical constituent minerals are mainly carbonate minerals, with minor biotite, magnetite and apatite. Magnetites often form banded structure of 4–8 mm in width.

(3) Carbonatitic breccia

The unit is distributed in the west of the sector as a small body.

The rocks are pale brown in colour and comprise breccias of alvikite and metabasalt with matrices of alvikitic materials.

Sizes of breccias of metabasalt are usually several to ten centimeters.

(4) Ferrocarbonatite

The unit is distributed in the north part of the sector as a group of small dykes (dyke swarm) and as separate dykes in the middle to east of the sector. The sizes of dykes of the former are usually several tens of centimeter in width and several to ten meters in length. The later is also small in size, and the maximum one confimed is 100 m long and 3 m wide.

These dykes occur in the peripheral zone of the South Ruri Carbonatite Complex in a macroscopic veiw and the relation is same as the case of the North Ruri Hill South Sector.

The rocks have undergone strong weathering and contamination by oxidation of iron oxide minerals, resulting in brown to dark brown, reddish brown and block in colour. Magnetites sometimes forming banded structure have almost changed to ferric iron oxide.

(5) Phonolite

The unit is distributed as a large single body about 300 m in diameter in the southwest corner of the sector.

The typical cone-shape which is a common form of volcanic necks of phonolite in the Ruri Hill area is not seen in the locality, but a part of the body is estimated to form a volcanic neck because it has intruded into the marginal places between carbonatite massive body and basement Nyanzian Metabasalt.

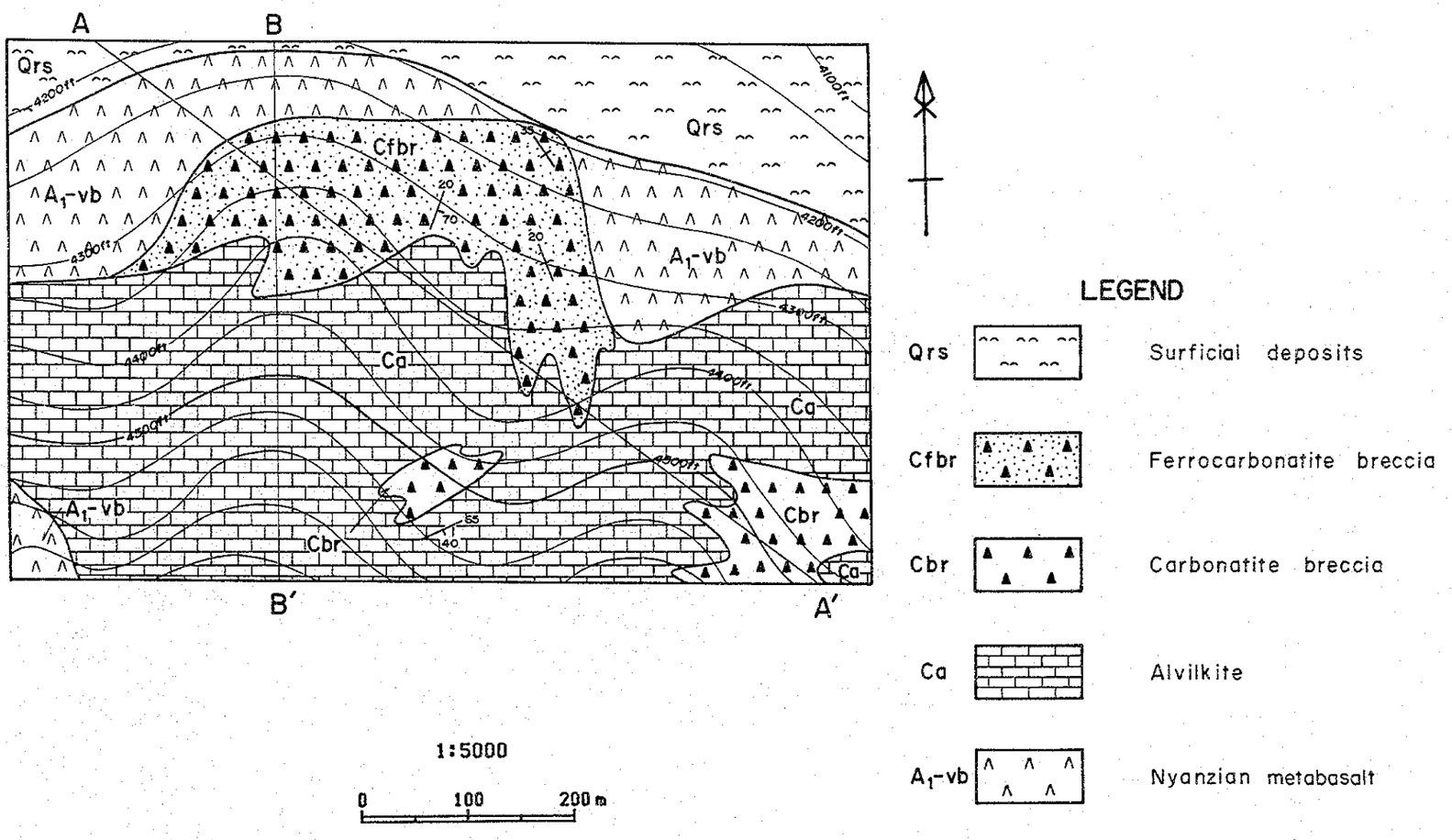

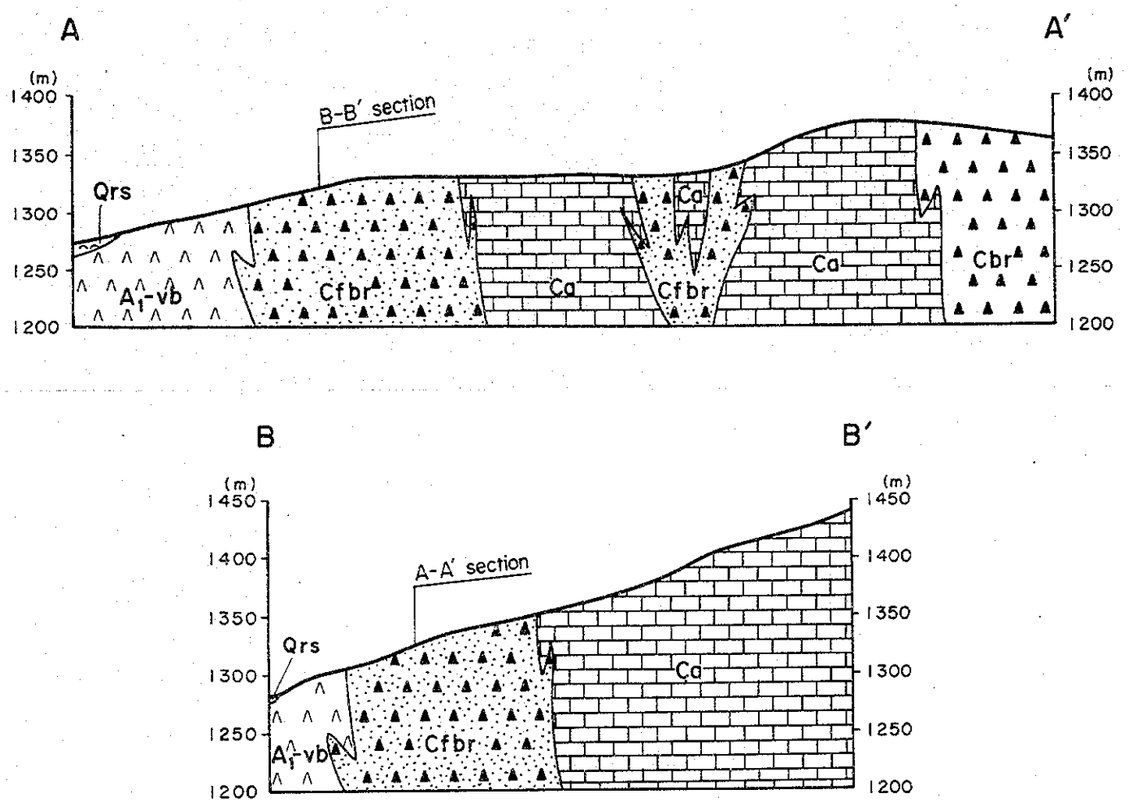

Fig. II – 1 – 3 Geological Map of the North Ruri Hill North Sector

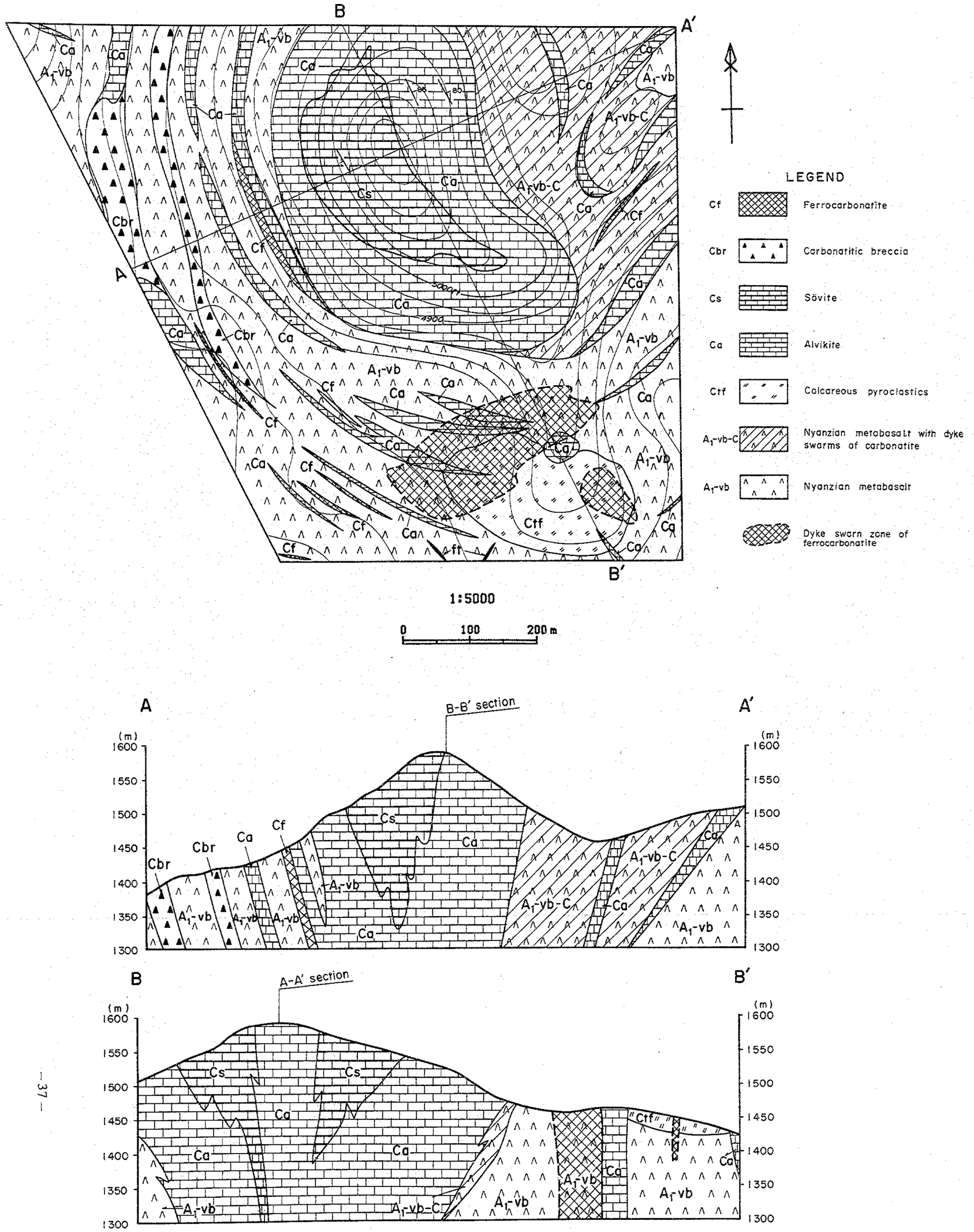

Fig. II – 1 – 4 Geological Map of the North Ruri Hill South Sector

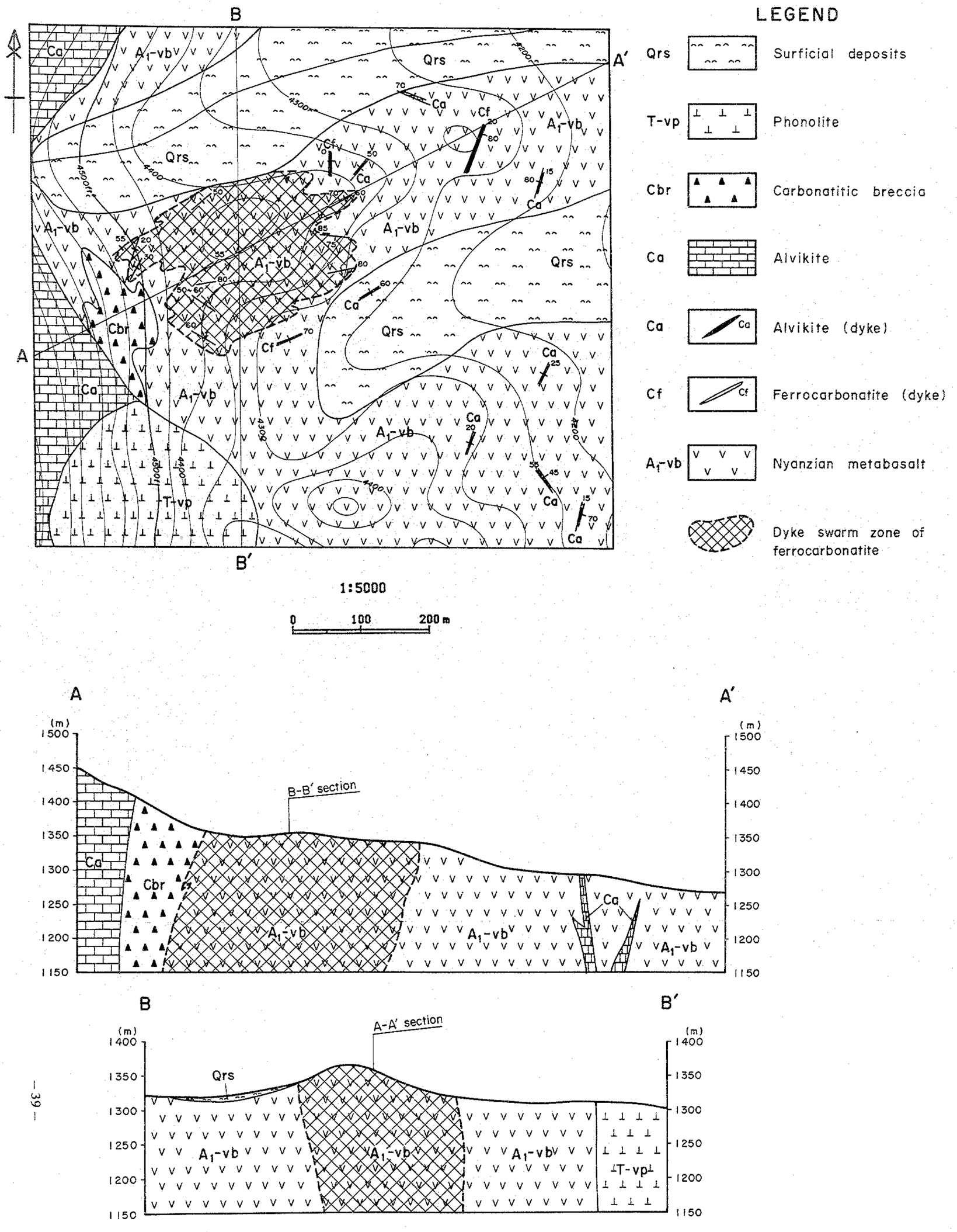

Fig. II – 1 – 5 Geological Map of the South Ruri Hill Sector

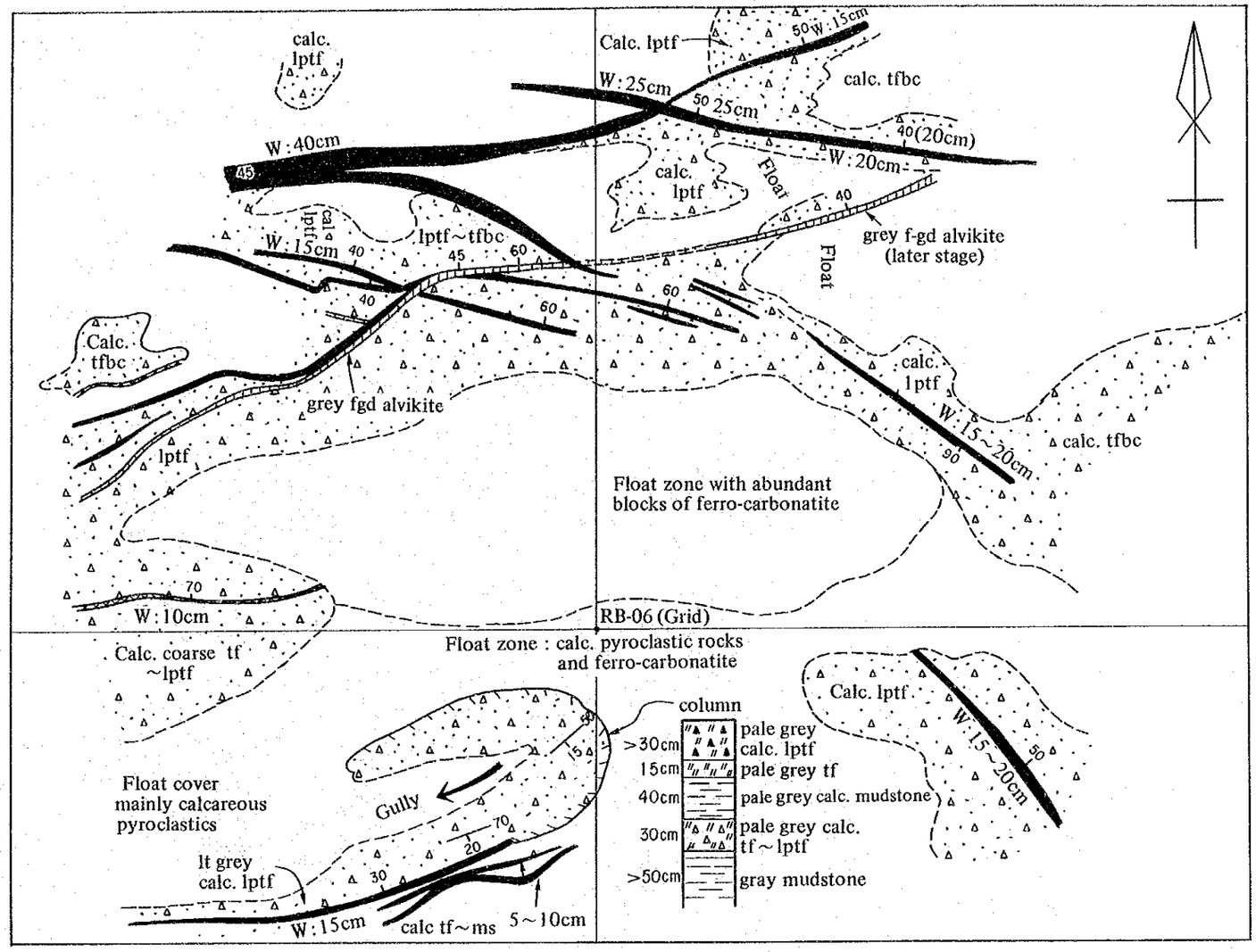

Fig. II – 1 – 6 Geological Sketch Map of the Dyke Swarm Zone of Ferrocarbonatite in the South Part of the North Ruri Hill South Sector

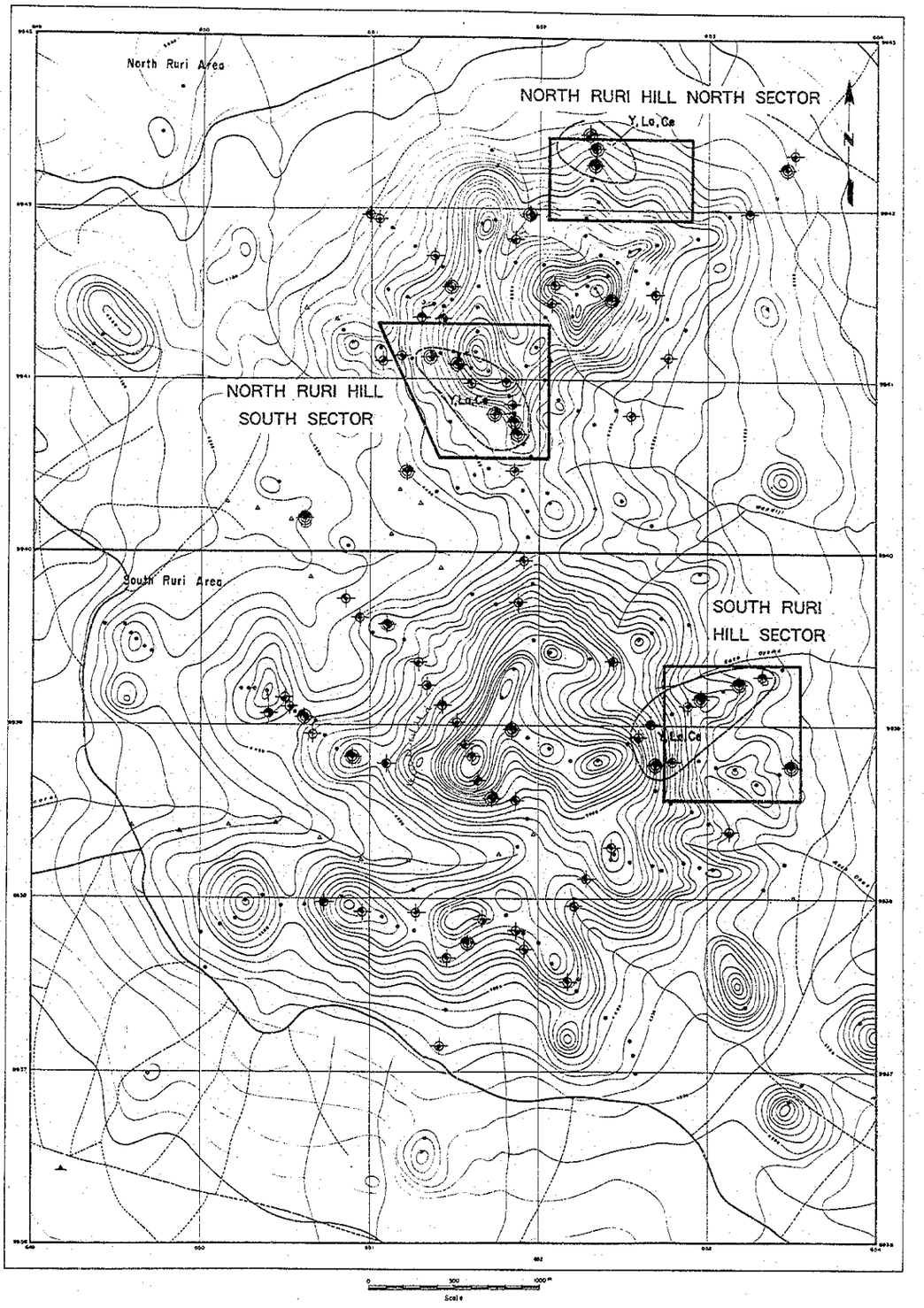

LEGEND

- Non anomalous sample
- Anomalous sample (≧ m + 1S , <m+2S)
- Highly anomalous sample (≧ m + 2S)
- Geochemicaly anomalous zone (Torget area)
- Soil sample

Classification

Element	Anomalous, ≧ m+1S, <m+2S	Highly anomalous ≧ m + 2S
La ppm	≧ 767 , < 3,300	≧ 3,300
Y ppm	≧ 148 , < 344	≧ 344
Nb ppm	≧ 620 , < 2,600	≧ 2,600
P %	≧ 0.61 , < 2.17	≧ 2.17

m : mean , S : standard deviation

Figures are of 1325 rock samples from all the Semi-detailed Survey Areas other than the grid-sampled areas in the Buru and Ndiru Hills.

Fig. II – 1 – 7 Location Map of Geochemical Survey Area in the North & South Ruri Hill Area
(Phase I Geochemical Results)

The rocks are grey to greenish grey and porphyritic, and contain phenocrysts of acicular hornblende, granular pyroxene, granular nepheline and tabular alkaline feldsper 10 mm in diameter. The groundmass is vitric and sometimes shows flow texture.

1–4 Results of Geochemical Exploration

The survey area comprising three sectors is shown in Fig. II–1–6 (Phase I results).

1–4–1 North Ruri Hill North Sector

Nine survey lines (A to I) at 100 m intervals were set in E–W direction and somples were collected at 50 m intervals along each survey line. Sampling was not done in areas where soil cover was very thick.

Total number of samples is 81 and the sampling points are shown in Apx 16.

(1) Univariate Analysis

The summary of statistics of geochemical analysis are shown in Table II–1–2.

Measn values for each element are all higher than that of "All the Area". This is caused that only one phonolite sample is included in the samples group analysed.

This is thought to be caused by a minor amount of noncarbonatitic rocks in the sample group. Non carbonatitic rocks are low in conterds of the analytical elements.

In maximum values of each element, 9 elements, paticularly 7 element in 8 REE represent also the maximum values of that of "All the Areas".

(2) Correlation analysis

The correlation coefficients among 16 components including γ–ray intensity are presented in Table II–1–3.

Strong correlations are observed among Ba, Y, Th and REE and the coefficients are all more than 0.6. The maximum coefficient is observed among Sm and Eu (0.990). Correlations among γ–ray intensity and these 11 element are also high (0.4–0.8), meanig mutual strong correlation of these 12 elements.

(3) Principal component analysis

Summary of the principal component analysis of major first four components is listed in Table II–1–4. The cumulative contribution of the four reaches 87%.

The first principal component (Z1) represents 61% of the total amount of information on the analytical data. Z1 is strongly affected by γ–ray Ba, Y, Th and REE, and from the elements Z1 is thought to represent the concentration of REE.

The second principal component represents 12% and is decided mainly by the value of Sr (factor loading 0.899), showing different behavior of Sr in REE concentration.

The third principal component represent 10% and is mainly decided by the value of P (factor loading 0.811) and partly by U (0.618).

The fourth principal component represent 6% and is decided by the value of Nb (factor loading 0.732).

Four elements; Sr, P, U and Nb which contribute highly in positive values to the second to fourth principal components have possibility to behave differently with other elements which represent REE concentration.

(4) Geochemically anomalous zones

Cumulative frequency distributions and Histograms of 9 components (P, Nb, Y, Th, La+Ce+Nd, Eu, Yb, γ-ray intensity, score of first component in the principal component analysis -z1) are shown in Apx 15, and the density maps with anamaly zones are shown in Apx 17 to 25.

Main anomaly zones are summarized as follows.

Y, Th, La+Ce+Nd, Eu, Yb: Distributions of anomaly zones and patters of contour in these 5 components are very similar and are covered by anomaly zone of scores of Z1.

Scores of Z1: The major anomaly zone covers the body of ferrocarbonatite breccia and the immediate periphery. It means Y, Th and REE are concentrated in the body. There are low value samples for the elements in the body, indicating heterogeneous character of the ferrocarbonatite body.

(5) Chondrite-normalized REE patterns

Six highest score samples for Z1 component are plotted on chondrite-normalized REE patterns (Fig. II-1-8). Five samples among six are ferrocarbonatite, and another is alvikite.

Negative anomaly of Ce and La (NE-06) and Ce, Nd and La (NC-10) are observed as a main characteristic in the sector.

From the chondrite-normalized REE patterns of ferrocarbonatite by suvey sector (average values of ferrocarbonatite are used, Fig. II-3-3), it has turned out that the ferrocarbonatites are rich in M $\sim$ HREE.

(6) Interpretation

In general, the rocks of the sector have higher values in 9 among 16 elements than that of other sectors, and the tendency is much strong in REE particularly in Tb, Yb and Lu.

Twelve elements; Eight REE, Ba, Y, Th and γ-ray intensity have turned out to be represented

Table II – 1 – 2 Summary of Statistics of Geochemical Analysis – North Ruri Hill North Sector –

Component	Unit	Number of sample	Max.	Min.	Mean (M)	Std.dev. (δ)	m+1 δ	m+2 δ	Threshold
γ –ray	cps	81	8943	356	1283	0.35	2889	6509	3200
P	%	81	2.860	0.027	0.211	0.50	0.661	2.071	0.560
Ba	ppm	81	36100	430	3700	0.43	9839	26161	
Sr	ppm	81	7020	292	2024	0.31	4143	8479	
Nb	ppm	81	2650	8	230	0.55	814	2889	880
Y	ppm	81	2300	13	174	0.44	484	1345	1000
U	ppm	81	51	0.5	5	0.61	21	84	
Th	ppm	81	2601	5	77	0.69	371	1302	1200
La	ppm	81	14330	44	596	0.51	1925	6215	
Ce	ppm	81	19470	83	1192	0.53	4023	13578	
Nd	ppm	81	5500	25	362	0.57	1334	4911	
Sm	ppm	81	826	4.7	61.1	0.50	193.0	610.1	
Eu	ppm	81	233	1.3	19.3	0.48	58.4	177.1	50
Tb	ppm	81	60.2	0.6	5.6	0.44	15.5	43.1	
Yb	ppm	81	113.0	0.7	7.7	0.46	22.2	64.4	49
Lu	ppm	81	16.0	0.05	1.2	0.45	3.4	9.5	
La+Ce+Nd	ppm	81	36640	156	2200	0.53	7428	25076	8000

Remarks : Standard deviation is shown in logarithmic scale.

Table II – 1 – 3 Correlation Coefficient – North Ruri Hill North Sector –

	γ –ray	P	Ba	Sr	Nb	Y	U	Th	La	Ce	Nd	Sm	Eu	Tb	Yb	Lu
γ –ray																
P	.021															
Ba	.670	.018														
Sr	-.317	.358	-.278													
Nb	.324	.013	.270	-.070												
Y	.776	.174	.756	-.051	.310											
U	.162	.298	.100	.132	.175	.199										
Th	.751	-.016	.744	-.154	.230	.889	.141									
La	.407	.040	.629	.313	.177	.698	.164	.634								
Ce	.445	-.017	.664	.266	.143	.704	.138	.685	.974							
Nd	.549	-.080	.706	.130	.151	.747	.108	.749	.885	.948						
Sm	.547	-.051	.685	.199	.185	.770	.091	.769	.879	.944	.966					
Eu	.590	-.006	.700	.182	.200	.821	.123	.798	.865	.928	.954	.990				
Tb	.648	.115	.687	.182	.243	.907	.167	.812	.825	.854	.878	.926	.955			
Yb	.747	.239	.717	-.016	.268	.960	.172	.800	.660	.658	.673	.708	.762	.855		
Lu	.719	.230	.730	.009	.303	.958	.178	.871	.703	.708	.710	.756	.804	.879	.980	

Table II – 1 – 4 Summary of Principal Component Analysis – North Ruri Hill North Sector –

Principal Compo.	Eigen Value	Contribution	Cumm. Contribut.	Item	γ-ray	P	Ba	Sr	Nb	Y	U	Th	La	Ce	Nd	Sm	Eu	Tb	Yb	Lu
1	9.685	0.605	0.61	Eigen vector	0.234	0.026	0.259	0.020	0.093	0.301	0.060	0.286	0.276	0.286	0.293	0.299	0.306	0.308	0.289	0.296
				Factor loading	0.727	0.079	0.805	0.063	0.289	0.935	0.188	0.891	0.860	0.891	0.911	0.930	0.952	0.960	0.898	0.921
				Contribution	0.528	0.006	0.648	0.004	0.083	0.875	0.035	0.795	0.740	0.793	0.830	0.864	0.906	0.921	0.807	0.848
2	1.836	0.115	0.72	Eigen vector	-0.366	0.208	-0.225	0.663	-0.209	-0.133	0.092	-0.191	0.267	0.245	0.138	0.160	0.132	0.086	-0.129	-0.095
				Factor loading	-0.496	0.282	-0.305	0.899	-0.284	-0.180	0.124	-0.258	0.362	0.331	0.187	0.217	0.178	0.117	-0.175	-0.128
				Contribution	0.246	0.080	0.093	0.808	0.081	0.032	0.015	0.067	0.131	0.110	0.035	0.047	0.032	0.014	0.030	0.016
3	1.532	0.096	0.82	Eigen vector	0.109	0.655	-0.044	0.159	0.229	0.145	0.499	-0.002	-0.115	-0.178	-0.214	-0.184	-0.129	0.011	0.195	0.174
				Factor loading	0.134	0.811	-0.054	0.197	0.284	0.179	0.618	-0.002	-0.142	-0.220	-0.265	-0.228	-0.159	0.013	0.241	0.216
				Contribution	0.018	0.657	0.003	0.039	0.081	0.032	0.382	0.000	0.020	0.048	0.070	0.052	0.025	0.000	0.058	0.047
4	0.918	0.057	0.87	Eigen vector	-0.039	-0.356	-0.017	0.041	0.764	-0.114	0.401	-0.111	0.113	0.093	0.073	0.063	0.034	-0.033	-0.210	-0.152
				Factor loading	-0.038	-0.341	-0.017	0.039	0.732	-0.109	0.384	-0.106	0.108	0.089	0.070	0.060	0.033	-0.031	-0.201	-0.146
				Contribution	0.001	0.116	0.000	0.002	0.536	0.012	0.147	0.011	0.012	0.008	0.005	0.004	0.001	0.001	0.040	0.021

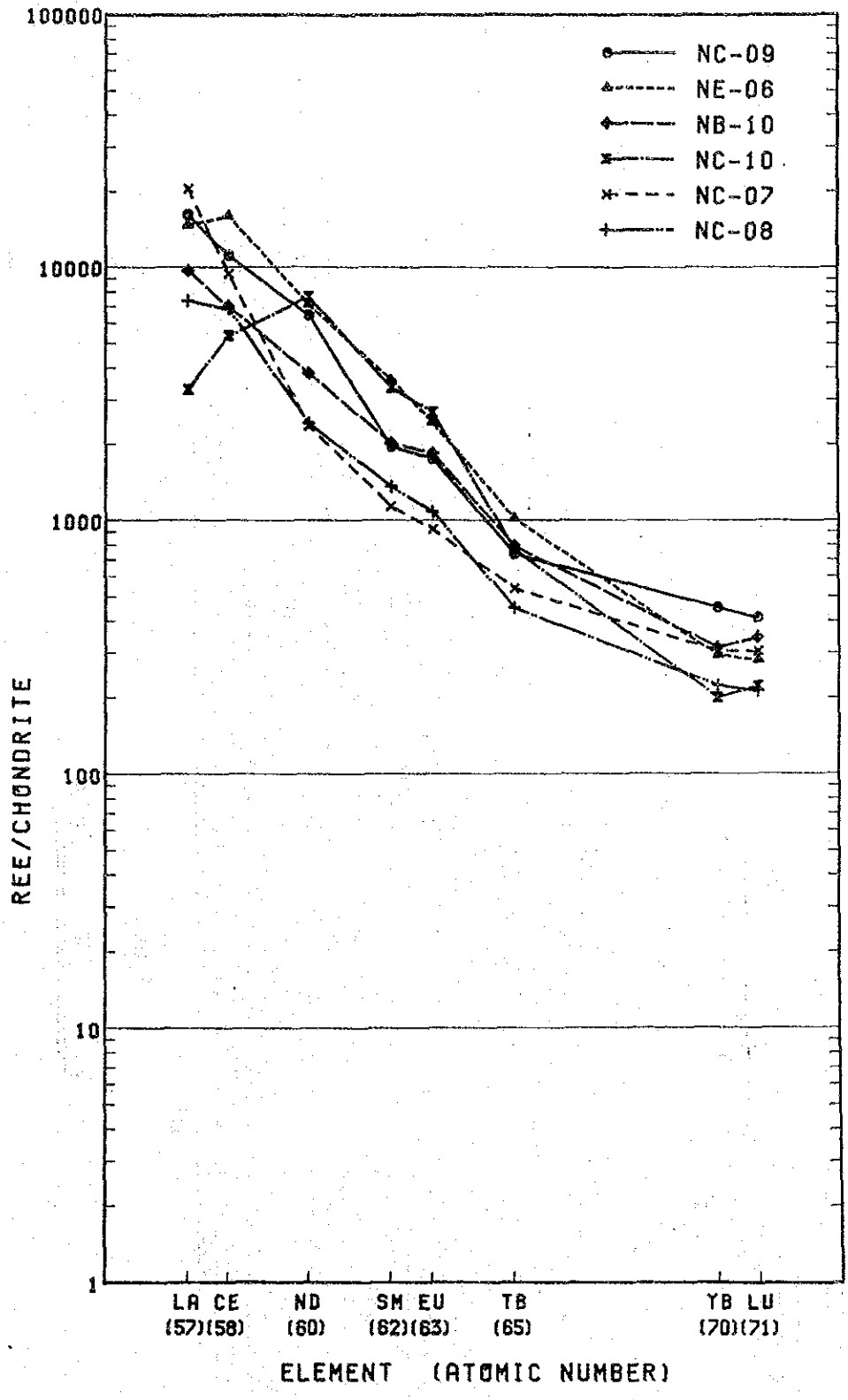

Fig. II – 1 – 8 Chondrite-Normalized REE Patterns, North Ruri Hill North Sector

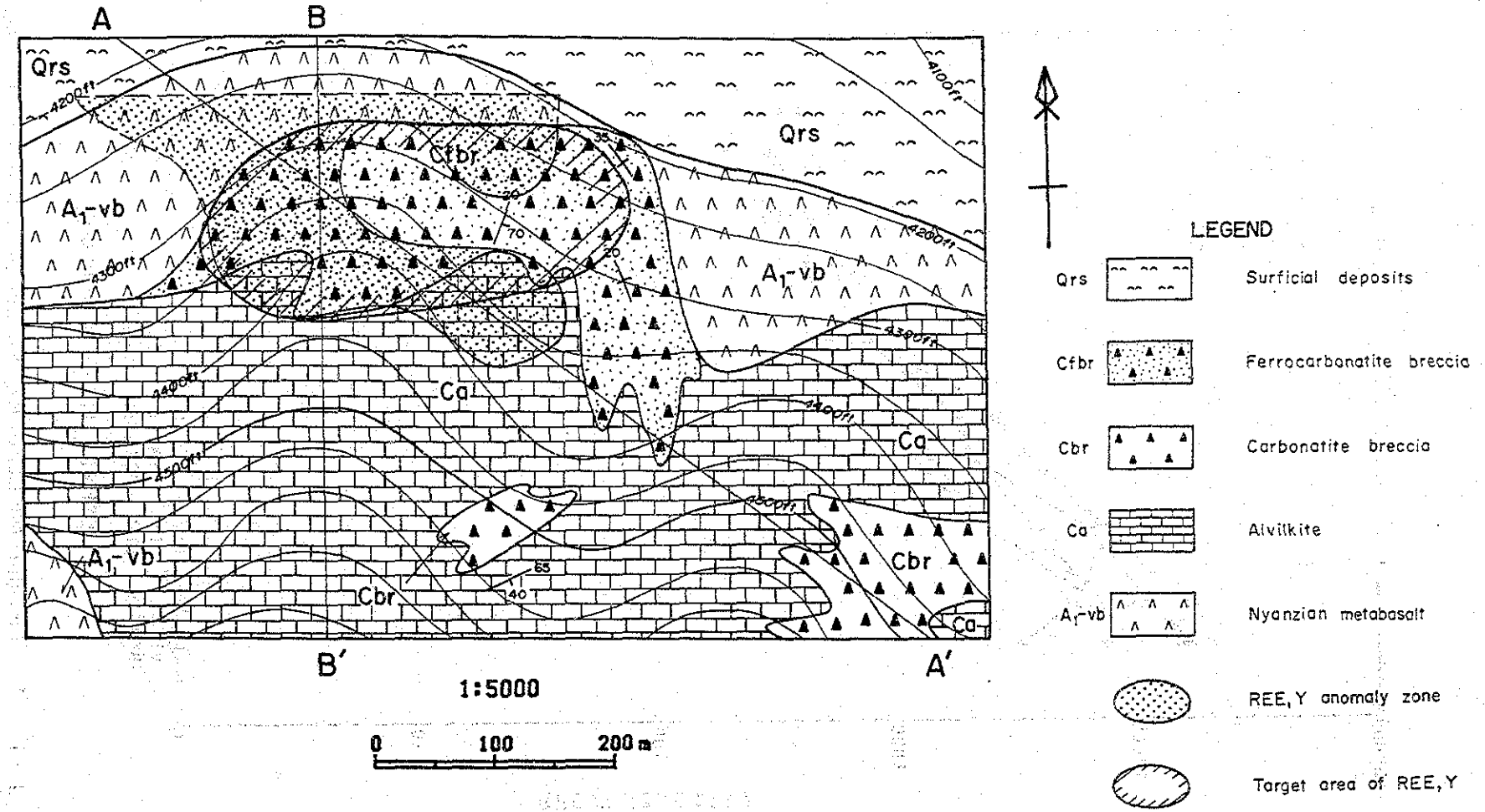

Fig. II – 1 – 9 Geochemical Interpretation Map, North Ruri Hill North Sector

by Z1 (the first principal component in principal component analysis) and it clearly represents the concentration of these elements. The major anomaly zone of score of Z1 covers the ferro-carbonatite body and the peripheyry located in the north of the sector, which means the body is a main target area of REE (Fig. II–1–9).

The chondrite-normalized REE patterns show that the concentration of M to HREE (Tb, Yb, Lu) is stronger than that of LREE (La, Ce).

1–4–2 North Ruri Hill South Sector

Nine survey lines (A to I) at 100 m intervals were set in N–S direction and samples were collected at 50 m intervals on each survey line.

Total number of samples are 150 and the sampling points are shown in Apx 27.

(1) Univariate Analysis

The summary of statistics of geochemical analysis are shown in Table II–1–5.

In comparing with the summary of "All the Areas" (Table II–3–1), values of elements of the rocks in the sector have following characters;

Means of REE except Lu, Sr and P are higher and of Ba are lower than that of the "All the Areas". Among these elements, the value of Sr is twice and P is one and half of that "of All the Areas", indicating that considerable amounts of sövite samples which are usually rich in Sr and P are included in the group of samples in this sector.

(2) Correlation analysis

The correlation coefficients among 16 components including γ–ray intensity are presented in Table II–1–6.

Strong correlations are observed among 12 elements (Ba, Y, Th, eight REE and γ–ray intensity) and the coefficients are all more than 0.6. The maximum coefficient is 0.990 among La and Ce.

Among other elements, there is a moderate coefficient in Nb–U (0.592), but any particular correlation is not observed.

(3) Principal component analysis

Summary of the principal component analysis of major first four components is listed in Table II–1–7.

The cumulative contribution of the four reaches 86%. The first principal component (Z1) represent 62% of the total amount of information on the analytical data. This is strongly affected by Ba, Y, Th, REE (La, Ce, Nd, Sm, Eu, Tb, Yb, Lu) and γ–ray intensity, and is thought to

Table II – 1 – 5 Summary of Statistics of Geochemical Analysis – North Ruri Hill South Sector –

Component	Unit	Number of sample	Max.	Min.	Mean (M)	Std.dev. (δ)	m+1 δ	m+2 δ	Threshold
γ –ray	cps	150	3430	183	765	0.22	1275	2126	1100
P	%	150	3.120	0.014	0.220	0.44	0.604	1.659	0.700
Ba	ppm	150	24000	310	2267	0.42	5968	15712	
Sr	ppm	150	12180	214	2793	0.27	5235	9814	
Nb	ppm	150	1850	2.5	129	0.57	480	1783	1000
Y	ppm	150	1100	21	135	0.36	309	708	350
U	ppm	150	247	0.5	5	0.59	18	69	
Th	ppm	150	941	0.5	55	0.60	219	870	160
La	ppm	150	12100	8	696	0.53	2380	8135	
Ce	ppm	150	19430	12	1216	0.50	3883	12401	
Nd	ppm	150	3910	7	321	0.44	883	2429	
Sm	ppm	150	341	2.4	49.1	0.38	117.6	281.5	
Eu	ppm	150	102	1.1	15.0	0.37	35.6	84.3	70
Tb	ppm	150	35.6	0.1	4.3	0.38	10.3	24.4	
Yb	ppm	150	51.7	1.3	6.1	0.36	13.9	31.7	40
Lu	ppm	150	6.2	0.1	0.4	0.36	2.1	4.7	
La+Ce+Nd	ppm	150	34270	27	2255	0.50	7165	22764	7000

Remarks : Standard deviation is shown in logarithmic scale.

Table II – 1 – 6 Correlation Coefficient – North Ruri Hill South Sector –

	γ –ray	P	Ba	Sr	Nb	Y	U	Th	La	Ce	Nd	Sm	Eu	Tb	Yb	Lu
γ –ray																
P	.099															
Ba	.654	-.002														
Sr	.265	.338	.219													
Nb	.176	.095	.143	.024												
Y	.734	.107	.711	.281	.084											
U	.466	.316	.409	.207	.592	.331										
Th	.782	-.055	.633	.231	.097	.841	.311									
La	.708	.069	.733	.349	.106	.832	.373	.807								
Ce	.704	.116	.694	.388	.141	.822	.398	.793	.990							
Nd	.682	.113	.633	.396	.158	.768	.391	.731	.953	.971						
Sm	.655	.097	.630	.360	.168	.816	.362	.735	.913	.934	.965					
Eu	.694	.115	.659	.358	.199	.869	.412	.765	.899	.922	.932	.976				
Tb	.698	.139	.645	.387	.189	.910	.377	.778	.832	.853	.843	.909	.951			
Yb	.685	.175	.662	.291	.049	.926	.306	.775	.725	.711	.644	.682	.739	.801		
Lu	.657	.152	.650	.265	.084	.886	.292	.754	.728	.710	.653	.694	.720	.754	.945	

Table II – 1 – 7 Summary of Principal Component Analysis – North Ruri Hill South Sector –

Principal Compo.	Eigen Value	Contribution	Cumm. Contribut.	Item	γ-ray	P	Ba	Sr	Nb	Y	U	Th	La	Ce	Nd	Sm	Eu	Tb	Yb	Lu
1	9.992	0.624	0.62	Eigen vector	0.255	0.046	0.243	0.125	0.061	0.295	0.147	0.273	0.298	0.299	0.290	0.293	0.300	0.295	0.271	0.267
				Factor loading	0.806	0.146	0.767	0.396	0.192	0.934	0.465	0.863	0.942	0.946	0.918	0.927	0.949	0.934	0.858	0.843
				Contribution	0.650	0.021	0.588	0.157	0.037	0.872	0.216	0.745	0.888	0.894	0.843	0.860	0.901	0.872	0.735	0.711
2	1.583	0.099	0.72	Eigen vector	0.037	0.452	-0.028	0.204	0.586	-0.118	0.585	-0.152	-0.068	-0.022	0.002	-0.023	0.001	-0.012	-0.108	-0.106
				Factor loading	0.046	0.568	-0.035	0.257	0.738	-0.149	0.736	-0.191	-0.086	-0.028	0.002	-0.029	0.001	-0.015	-0.136	-0.134
				Contribution	0.002	0.323	0.001	0.066	0.544	0.022	0.542	0.037	0.007	0.001	0.000	0.001	0.000	0.000	0.019	0.018
3	1.202	0.075	0.80	Eigen vector	-0.116	0.579	-0.169	0.589	-0.446	0.003	-0.218	-0.134	-0.005	0.028	0.037	0.020	0.000	0.037	0.071	0.041
				Factor loading	-0.127	0.635	-0.185	0.646	-0.489	0.003	-0.239	-0.147	-0.005	0.030	0.040	0.022	0.000	0.041	0.078	0.045
				Contribution	0.016	0.403	0.034	0.417	0.240	0.000	0.057	0.021	0.000	0.001	0.002	0.000	0.000	0.002	0.006	0.002
4	0.918	0.057	0.86	Eigen vector	0.181	0.302	0.135	-0.247	-0.061	0.224	0.095	0.111	-0.205	-0.246	-0.349	-0.297	-0.202	-0.052	0.441	0.414
				Factor loading	0.173	0.289	0.130	-0.236	-0.058	0.214	0.091	0.107	-0.197	-0.235	-0.334	-0.285	-0.193	-0.050	0.423	0.397
				Contribution	0.030	0.084	0.017	0.056	0.003	0.046	0.008	0.011	0.039	0.055	0.112	0.081	0.037	0.002	0.179	0.158

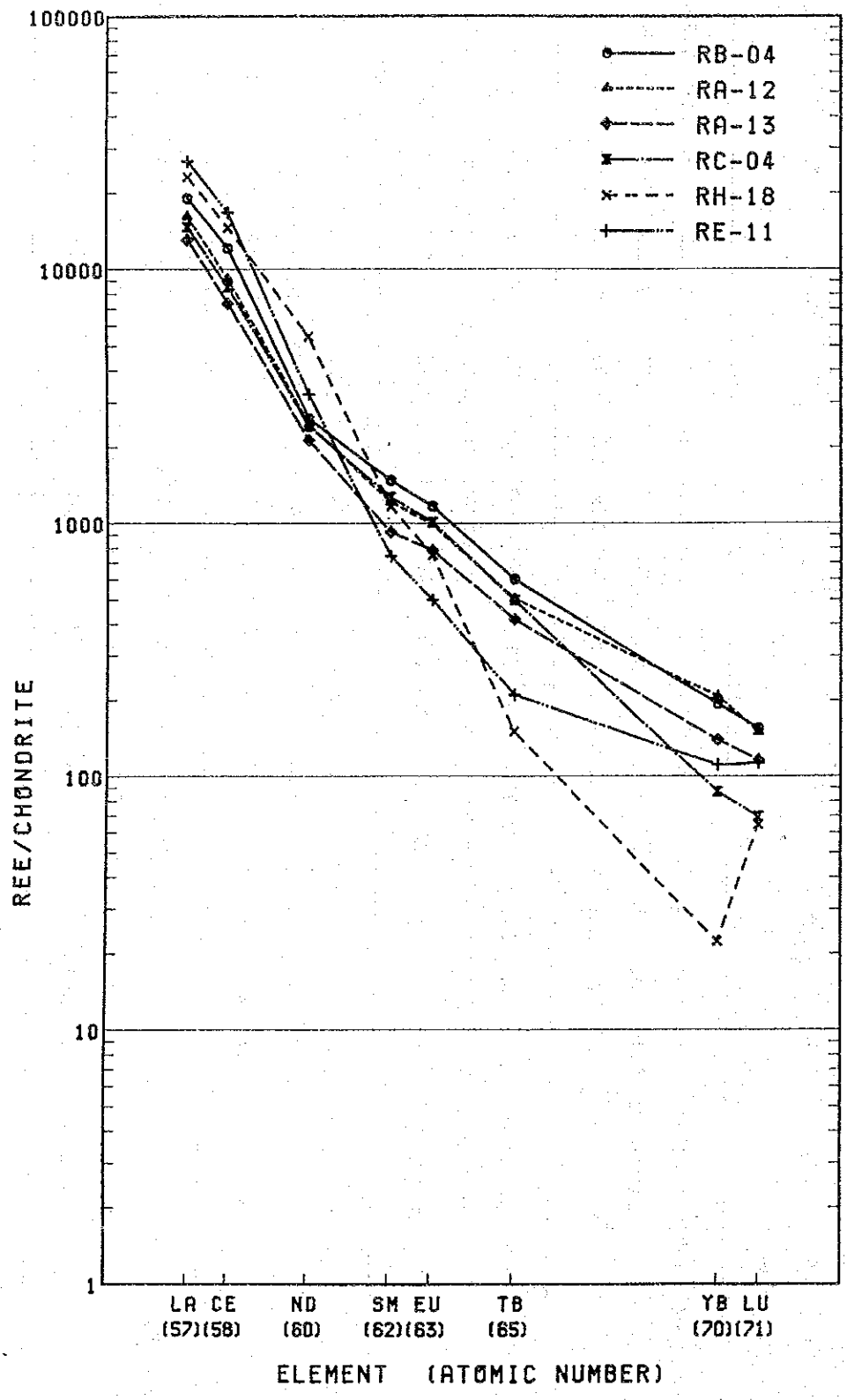

Fig. II – 1 – 10 Chondrite-Normalized REE Patterns, North Ruri Hill South Sector

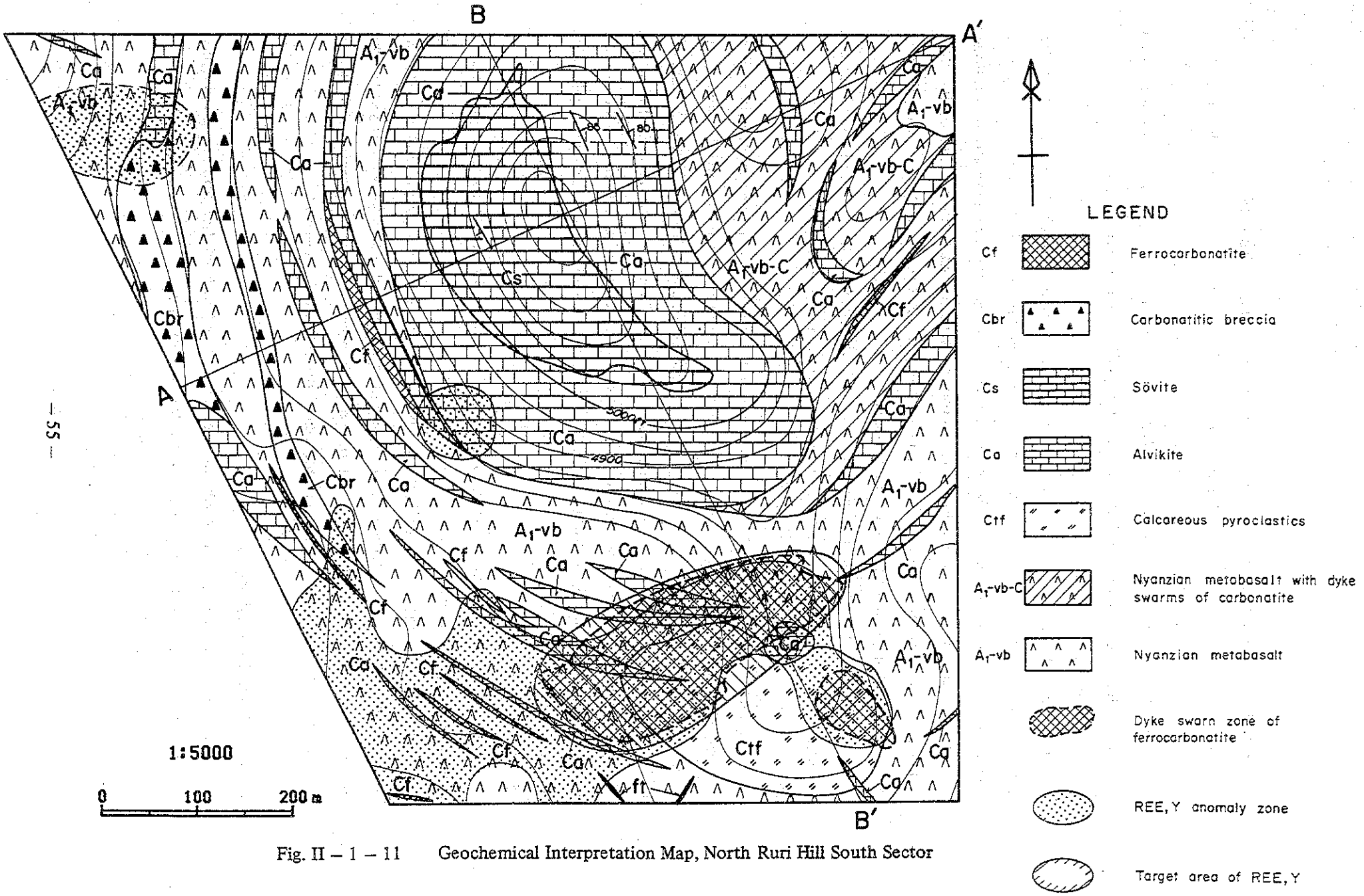

Fig. II – 1 – 11 Geochemical Interpretation Map, North Ruri Hill South Sector

represent the concentration of these elements relating to carbonatite activity.

The second is affected by P, Nb and U and the third by P and Sr, indicating the occurrence of sövite in a wider area than in other sectors.

The fourth is weakly affected by HREE (Yb, Lu), indicating possibility of somewhat different behavior of HREE (Yb, Lu) from the other REE in their concentration.

(4) Geochemically anomalous zones

Cumulative frequency distributions and histgrams of 9 components (P, Nb, Y, Th, La+Ce+Nd, Eu, Yb, γ-ray intensity and score of Z1) are shown in Apx 26, and the density maps with anamalous zones are shown in Apx 28 to 36. Main anomalous zones are summarized as follows;

Y, Th, La+Ce+Nd: Distributions and contour patterns of anomalous zones of the three components are very similar and in consistent with that of scores of Z1 covering the overlapping parts of anomalous zones of the three components.

Score of Z1: Major anomalous zones are widely distributed in the south of the sector and samples which have anomalous value to the score of Z1 are ferrocarbonatite.

(5) Chondrite-normalized REE patterns

Six highest score samples for Z1 component are plotted on a chondrite-normalized REE patterns (Fig. II-1-10). Four samples are ferrocarbonatite and two are alvikite among six samples. The patterns, show that the rocks are rich in LREE, somewhat rich in HREE and poor in MREE One sample (RH-18) has negative anomaly of Yb. Chondtrite-normalized REE pattern of ferrocarbonatite by survey sector (average values of ferrocarbonatite, Fig. II-3-3) also show the ferrocarbonatites in the sector are rich in La and Ce (paticularly in La), somewhat rich in Yb and Lu, and poor in Sm and Eu.

(6) Interpretation

High contents of samples in Sr and P are caused by the existence of a sövite body and La and Ce by ferrocarbonatites.

Twelve components (eight REE, Ba, Y, Th and γ-ray intensity) are represended by Z1 and the main anomalous zone of score of Z1 is situated in the south of the sector where dyke swarms of ferrocarbonatite occur. Distribution of anomalous zone of REE are overlapping with that of score of Z1, indicating to be the main target area of the sector (Fig. II-1-11).

1-4-3 South Ruri Hill Sector

Nine survey lines (A to I) at 100 m intervals were set in N-S direction and geochemical samples (rock) were collected at 50 m intervals along survey lines.

Sampling was not done in two areas along creek where debris and soil covers were very thick.

Total number of samples is 93 and the sampling points are shown in Apx 38.

(1) Univariate analysis

The summary of statistics of geochemical analysis are shown in Table II–1–8.

All mean values for each element are lower than that of "All the Areas". This is due to the proportion of samples that metabasalts which are low in these analytical elements occupy 40% of total samples, whereas 10% in "All the Areas".

The proportion of samples is also observed as two different pupulations in Apx 37.

(2) Correlation analysis

The correlation coefficients among 16 components including γ–ray intensity are presented in Table II–1–9.

Almost all the coefficients among 16 components exceed 0.6, and the maximum is 0.995 in Sm–Eu, minimum 0.468 in P–U.

This phenomenon which is not observed in other sectors is also due to the mixture of two different populations (carbonatite population and metabasalt one).

Comparably lower coefficients under 0.7 are seen between two elements in P, Nb, U and

(3) Principal component analysis

Summary of the principal component analysis of major first four components is listed in Table II–1–10.

The cumulative contribution of the four reaches 94% and it is the highest ratio in all sectors.

The first principal component (Z1) represent 79% of the total amount of information on the analytical data.

All 16 elements, contribute to the Z1 and it is thought to be strongly attected by the mixture of two different populations, though the concentration of REE is also thought to be represented by the components.

The second is weakly affected by P and Nb, which is similar to that of North Ruri Hill South Sector.

The third is affected by Yb and Lu, showing somewhat different behaiver of HREE from other REE .

The fourth is mainly affected by U.

(4) Geochemically anomalous zones

Cumulative frequency distributions and histgrams of 9 components (P, Nb, Y, Th, La+Ce+Nd, Eu, Yb, γ–ray intensity, score of Z1) are shown in Apx 37, and the density maps with anomalous

Table II – 1 – 8 Summary of Statistics of Geochemical Analysis – South Ruri Hill Sector –

Component	Unit	Number of sample	Max.	Min.	Mean (M)	Std.dev. (δ)	m+1 δ	m+2 δ	Threshold
γ –ray	cps	93	5535	75	501	0.53	1707	5822	2000
P	%	93	1.520	0.014	0.060	0.54	0.207	0.716	0.560
Ba	ppm	93	16660	170	1652	0.69	8002	38752	
Sr	ppm	93	5580	92	395	0.52	1299	4269	
Nb	ppm	93	2750	2.5	23	0.79	142	879	400
Y	ppm	93	700	16	72	0.54	250	873	500
U	ppm	93	22	0.5	2	0.55	9	24	
Th	ppm	93	2068	0.5	32	1.22	518	8513	1200
La	ppm	93	7960	3	170	1.11	2176	27899	
Ce	ppm	93	12250	7	331	1.10	4147	51918	
Nd	ppm	93	2860	2.5	112	1.03	1209	13051	
Sm	ppm	93	523	1.5	24.6	0.85	175.5	1251.5	
Eu	ppm	93	159.5	0.5	7.5	0.82	49.8	330.2	65
Tb	ppm	93	22.3	0.1	2.0	0.75	11.2	63.3	
Yb	ppm	93	41.1	0.1	3.9	0.44	10.6	28.9	15.5
Lu	ppm	93	6.2	0.2	0.7	0.36	1.7	3.9	
La+Ce+Nd	ppm	93	22050	14	657	1.03	7934	95887	5400

Remarks : Standard deviation is shown in logarithmic scale.

Table II – 1 – 9 Correlation Coefficient – South Ruri Hill Sector –

	γ –ray	P	Ba	Sr	Nb	Y	U	Th	La	Ce	Nd	Sm	Eu	Tb	Yb	Lu
γ –ray																
P	.513															
Ba	.918	.601														
Sr	.668	.834	.770													
Nb	.575	.822	.647	.703												
Y	.823	.698	.882	.840	.676											
U	.631	.468	.699	.569	.581	.664										
Th	.882	.568	.914	.714	.599	.889	.680									
La	.734	.652	.856	.809	.681	.853	.699	.905								
Ce	.807	.640	.913	.809	.672	.880	.720	.942	.985							
Nd	.876	.611	.954	.797	.649	.900	.696	.951	.907	.955						
Sm	.871	.627	.934	.799	.636	.913	.692	.970	.916	.957	.979					
Eu	.879	.634	.933	.804	.638	.925	.696	.970	.909	.950	.970	.995				
Tb	.814	.656	.866	.797	.646	.911	.663	.890	.860	.889	.891	.921	.933			
Yb	.596	.547	.610	.660	.521	.848	.487	.693	.670	.667	.642	.685	.706	.742		
Lu	.606	.536	.664	.640	.522	.868	.565	.747	.745	.732	.680	.722	.741	.769	.932	

Table II — 1 — 10 Summary of Principal Component Analysis — South Ruri Hill Sector —

Principal Compo.	Eigen Value	Contribution	Cumm. Contribut.	Item	γ-ray	P	Ba	Sr	Nb	Y	U	Th	La	Ce	Nd	Sm	Eu	Tb	Yb	Lu
1	12.578	0.786	0.79	Eigen vector	0.245	0.205	0.264	0.244	0.210	0.271	0.209	0.267	0.264	0.271	0.270	0.273	0.275	0.265	0.218	0.228
				Factor loading	0.868	0.726	0.937	0.867	0.744	0.961	0.740	0.948	0.936	0.961	0.959	0.970	0.974	0.940	0.774	0.808
				Contribution	0.754	0.528	0.877	0.752	0.553	0.923	0.548	0.900	0.876	0.924	0.919	0.940	0.949	0.884	0.599	0.654
2	1.031	0.064	0.85	Eigen vector	-0.244	0.599	-0.169	0.352	0.518	0.027	-0.079	-0.230	-0.028	-0.098	-0.164	-0.159	-0.150	-0.046	0.111	0.039
				Factor loading	-0.248	0.608	-0.172	0.357	0.526	0.028	-0.080	-0.233	-0.029	-0.100	-0.167	-0.162	-0.152	-0.047	0.113	0.040
				Contribution	0.062	0.370	0.030	0.128	0.277	0.001	0.006	0.054	0.001	0.010	0.028	0.026	0.023	0.002	0.013	0.002
3	0.869	0.054	0.90	Eigen vector	-0.142	-0.132	-0.179	-0.093	-0.239	0.194	-0.171	-0.021	-0.056	-0.098	-0.151	-0.081	-0.050	0.059	0.635	0.588
				Factor loading	-0.132	-0.123	-0.167	-0.087	-0.223	0.181	-0.159	-0.020	-0.052	-0.091	-0.140	-0.075	-0.047	0.055	0.592	0.548
				Contribution	0.017	0.015	0.028	0.007	0.050	0.033	0.025	0.000	0.003	0.008	0.020	0.006	0.002	0.003	0.351	0.300
4	0.491	0.031	0.94	Eigen vector	-0.154	-0.131	-0.083	-0.171	0.152	-0.061	0.904	-0.077	0.055	0.011	-0.108	-0.117	-0.111	-0.085	0.028	0.155
				Factor loading	-0.108	-0.092	-0.058	-0.120	0.107	-0.043	0.633	-0.054	0.038	0.008	-0.076	-0.082	-0.077	-0.060	0.020	0.109
				Contribution	0.012	0.008	0.003	0.014	0.011	0.002	0.401	0.003	0.001	0.000	0.006	0.007	0.006	0.004	0.000	0.012

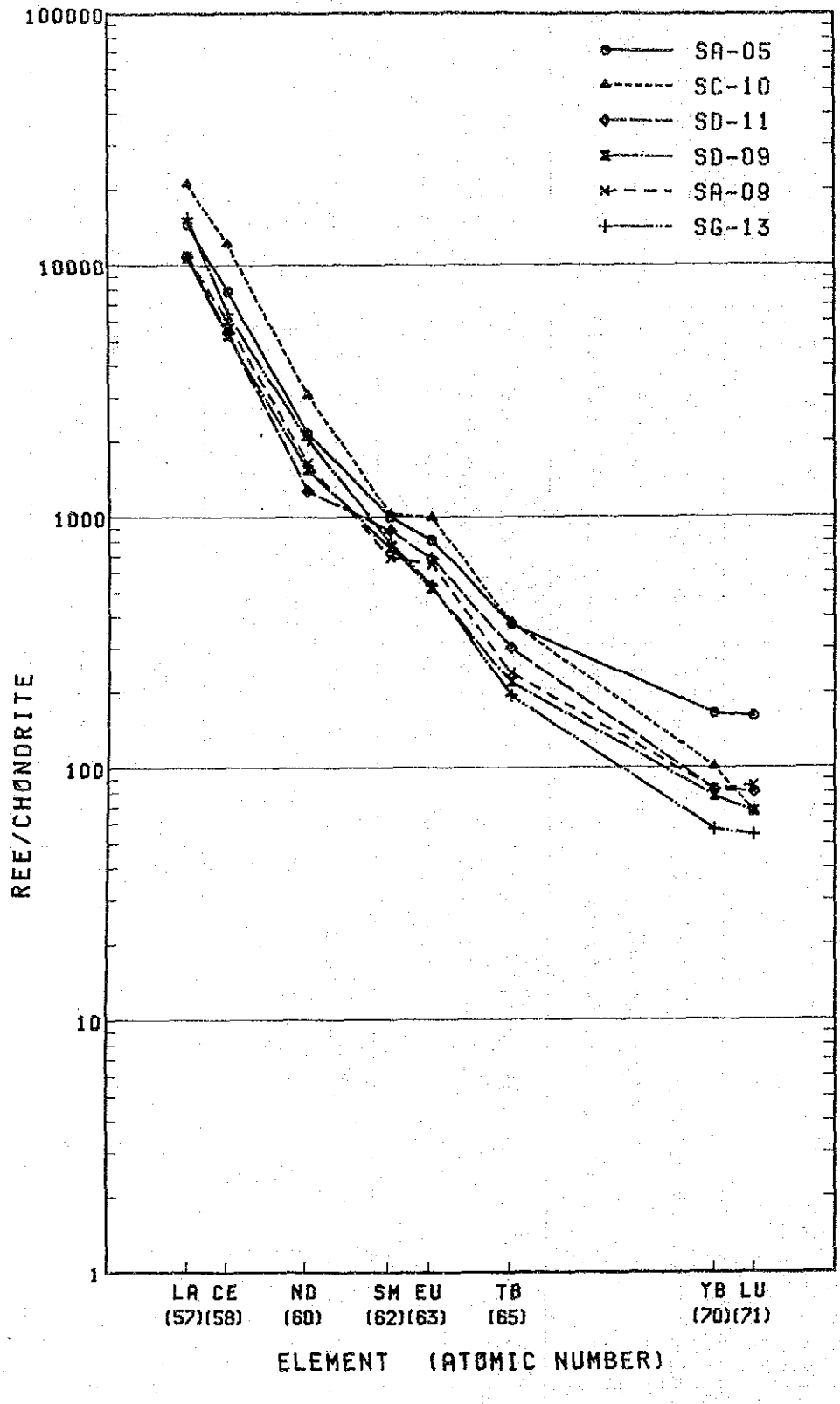

Fig. II – 1 – 12 Chondrite-Normalized REE Patterns, South Ruri Hill Sector

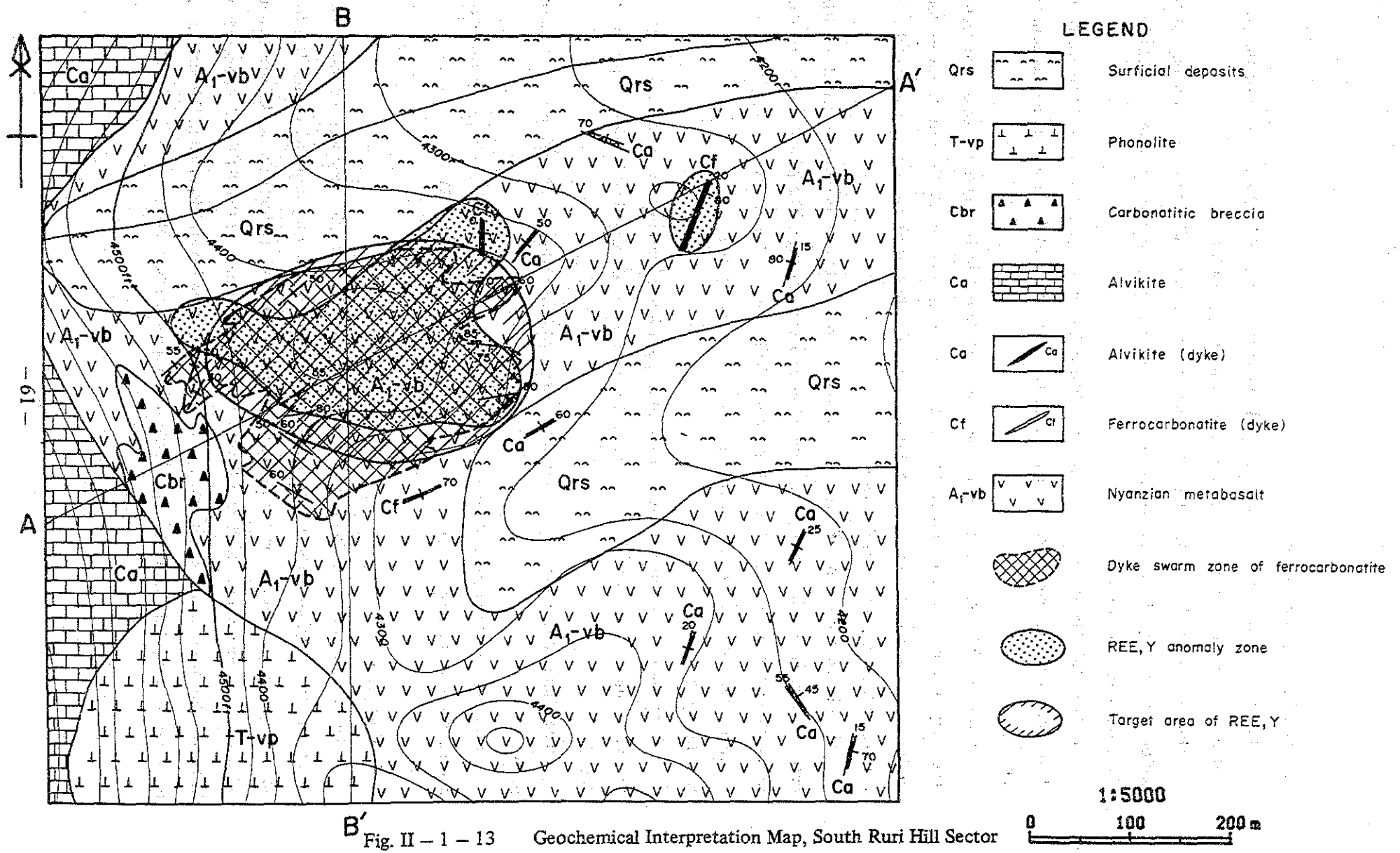

Fig. II – 1 – 13 Geochemical Interpretation Map, South Ruri Hill Sector

zones are shown in Apx 39–47.

P, Nb Y: Anomalous zones in these elements are dispersed in the west half of the sector and only anomalous zones of Y are included in that of La+Ce+Nd.

Eu, Th: Anomalous zones of the two elements are also distributed in the west half of the sector and the anomalous zones of Th all of which samples are ferrocarbonatite are included in the anomalous zones of Eu.

La+Ce+Nd: Major anomalous zones are distributed in the central part of the sector where dyke swarms of ferrocarbonatites occur. These zones also inclued the major anomalous zones of Yb.

Scores of Z1: Major anomalous zones are distributed in the central part of the sector. The samples which show anomaly are ferrocarbonatite except one sample. Refering to the geology of the area, the contour line of score 0 devides the distribution of carbonatite and metabasalt.

(5) Chondrite-normalized REE patters

Six highest score samples for Z1 component are plotted on chondrite-normalized REE patterns (Fig. II–1–12). All samples plotted are ferrocarbonatite. The patterns show that the ferrocarbonatites are rich in REE and poor in HREE. This is also observed in Fig. II–3–3 in-which average values of ferrocarbonatite in all sectors are compared.

(6) Interpretation

Major anomalous zones related to the mineralization of carbonatite are almost limited in the major anomalous zone of La+Ce+Nd and the scores of Z1 and they include that of Y, Eu and Tb.

The major zone is located in the central part of the area where dyke swarms of carbonatite occur.

From the comprehensive study of geology and geochemistry of the sector, only the major anomalous zone is thought to be a target area of the sector (Fig. II–1–13).

1–5 Discussion

The three sectors where geological survey and geochemical exploration were conducted are situated in the marginal parts and the peripheries of the carbonatite complexes of the Ruri Hill, and the geology comprises basement Nyanzian Metabasalt and carbonatitic rocks which have intruded the former. From geochemical explorations it has turned out that REE and Y concentrate in ferrocarbonatite, on the other hand, high value samples in Nb are dispersed in the sectors and not depend on the distribution of a particular rock type of carbonatites.

1–5–1 North Ruri Hill North Sector

The body of ferrocarbonatitic breccia is distributed in the center of the sector in an area of 0.03 km^2 trending E–W direction. The rocks are heterogeneous in chemical contents and strongly weathered. Geochemically anomalous zones of REE and Y are distributed almost in the same area covering the body and the immediate periphery. The anomalous zone has low contents parts of these elements, suggesting the hetergeneous character of the body.

Chondrite-normalized REE patterns show ferrocarbonatites in the sector are rich in M to HREE, and poor in LREE, paticularly in La and Ce. The small size of the anomalous zone and the heterogeneous character of the rocks can't warrant any further exploration.

1–5–2 North Ruri Hill South Sector

Ferrocarbonatites are mainly distributed in the south of the sector in an area of 0.03 km^2 as dyke swarms which have intruded into alvikite, calcareous pyroclastics and basement rocks. The size of the dykes are usually several cm to 1 m in width and several to several tens of meters in length.

Major geochemically anomalous zones are that of Y, Th, La+Ce+Nd covering the zone of dyke-swarms of ferrocarbonatite and trending in E–W direction. The anomalous zones of the elements can be represented by the anomalous zone of score of Zl in the principal components analysis and the area is 0.06 km^2.

Chondrite-normalized REE patterns show that the ferrocarbonatites in the area are rich in La and Ce.

From the results of geology and geochemistry the anomalous zone is not a potential target area for REE and Y, though the area is larger than other two sectors.

1–5–3 South Ruri Hill Sector

Ferrocarbonatites in the sector occur as dykes or small dyke swarms and the majority occurs in the center to northwest part of the sector.

Major geochemically anomalous zone of the sector is seen only in La+Ce+Nd covering the zone of dyke swarms of ferrocarbonatite.

Chondrite-normalized REE patterns show the ferrocarbonatites in the zone are somewhat rich in La and Ce.

Results of geological and geochemical explorations show a low potentiality for concentration of REE and Y in the sector.

CHAPTER 2 KUGE–LWALA AREA

2–1 Methods of survey

Both geological survey and geochemical exploration in the area were conducted in a same way as in the North & South Ruri Hill Area. Some different points are as follows.

Geological survey : Trench survey was practiced in the area to know the mode of occurrence of carbonatites. The length is 120 m (3 localities) in the Kuge Sector and 200 m (one locality) in the Lwala Sector.

Geochemical exploration : Survey lines were set at 50 m intervals and sampling was done on 50 m x 50 m grids.

2–2 General Geology

In the Wasaki Peninsula to the west of the town of Homa Bay, ijolite and carbonatite bodies are known to be distributed at several localities. The Kuge-Lwala Area located at the southwest end of the peninsula includes small carbonatite bodies at Kuge Hill and Lwala.

The body at Kuge Hill is a cone-sheet of carbonatite, close to which a ferrocarbonatite dyke occurs. The cone-sheet seems to express the top of an intrusive, so that a massive body may be expected at the depths. The ferrocarbonatite dyke is 30 to 40 m wide and more than 450 m long in a N-S direction dipping to the west.

The body at Lwala is mainly comprises ferruginous breccias which contain carbonatitic fragments. It outcrops in an area of about 0.3 km^2.

The geological plan and profiles are shown in Fig. II–2–1 (Phase I results).

2–3 Results of Geological Survey

Generalized geological columner sections are presented in Fig. II–2–2.

2–3–1 Kuge Sector

The sector involves a rolling hill at Kuge and the peripheral flats. The geology of the sector comprises basement Nyanzian Metabasalt, alvikite and ferrocarbonatite. The main structure of carbonatite is a semi-circular one opening at the southwest of the Hill.

The geological plan and profiles of the sector are shown in Fig. II–2–3.

(1) Nyanzian Metabasalt

The unit is distributed in the southern and western parts of the sector and in the area of the top of the Kuge Hill. The later occurs as a roof on the carbonatite body of Kuge Hill and have

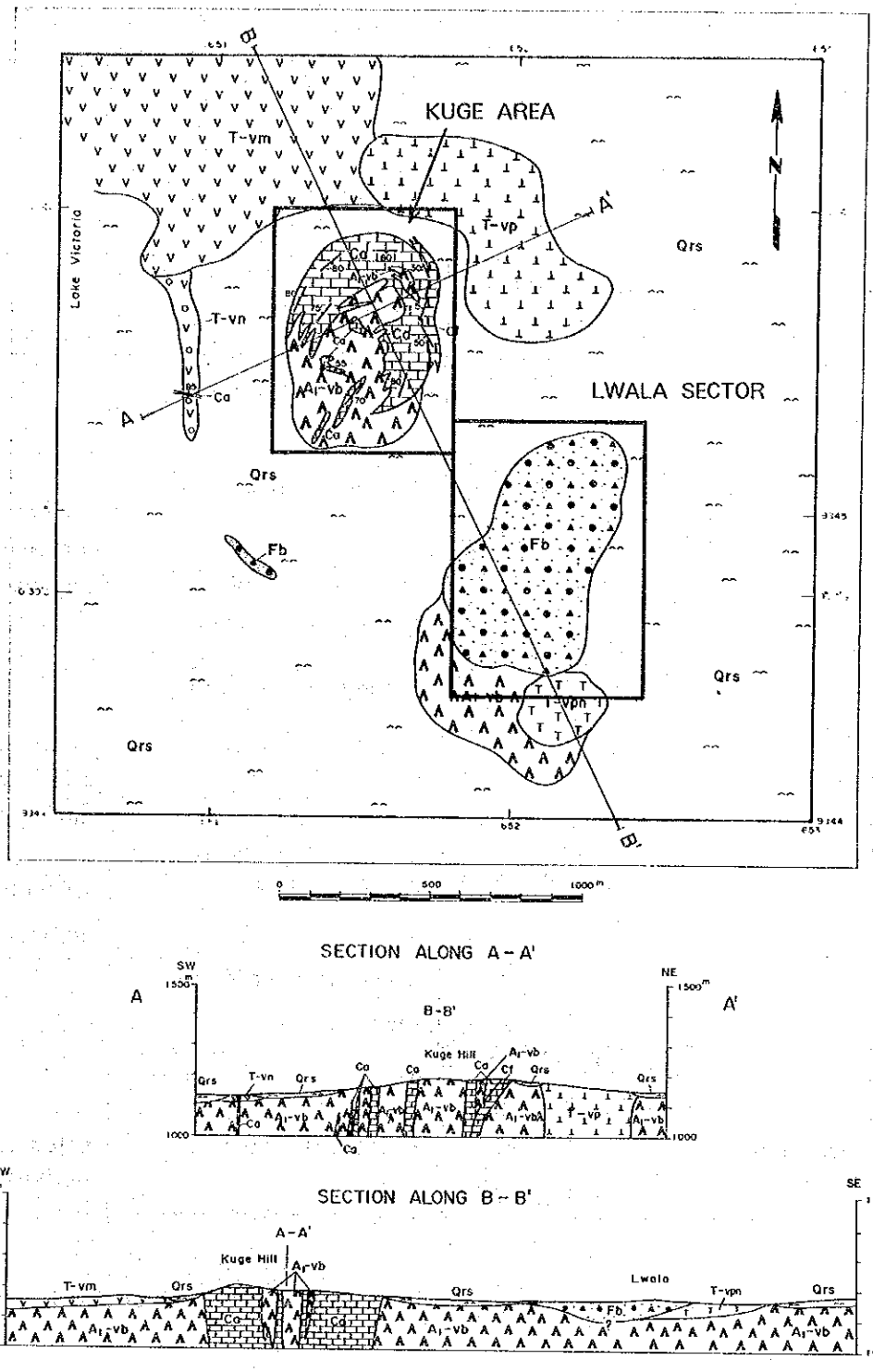

LEGEND

Qrs		Surficial deposits
Fb		Ferrugious breccia
Cf		Ferrocarbonatite
Ca		Alvikite
T-vpn		Phonolitic nephelinite
T-vp		Porhyritic phonolite
T-vm		Olivine melanephelinite
T-vn		Nephelinite, agglomerate
A1-vb		Nyanzian metabasalt

Strike and dip of beddiug

Strike and dip of flow banding

Dykes and sheets with dip

A——A' Line of section

Fig. II – 2 – 1 Geological Map of the Kuge-Lwala Area (Phase I Results)

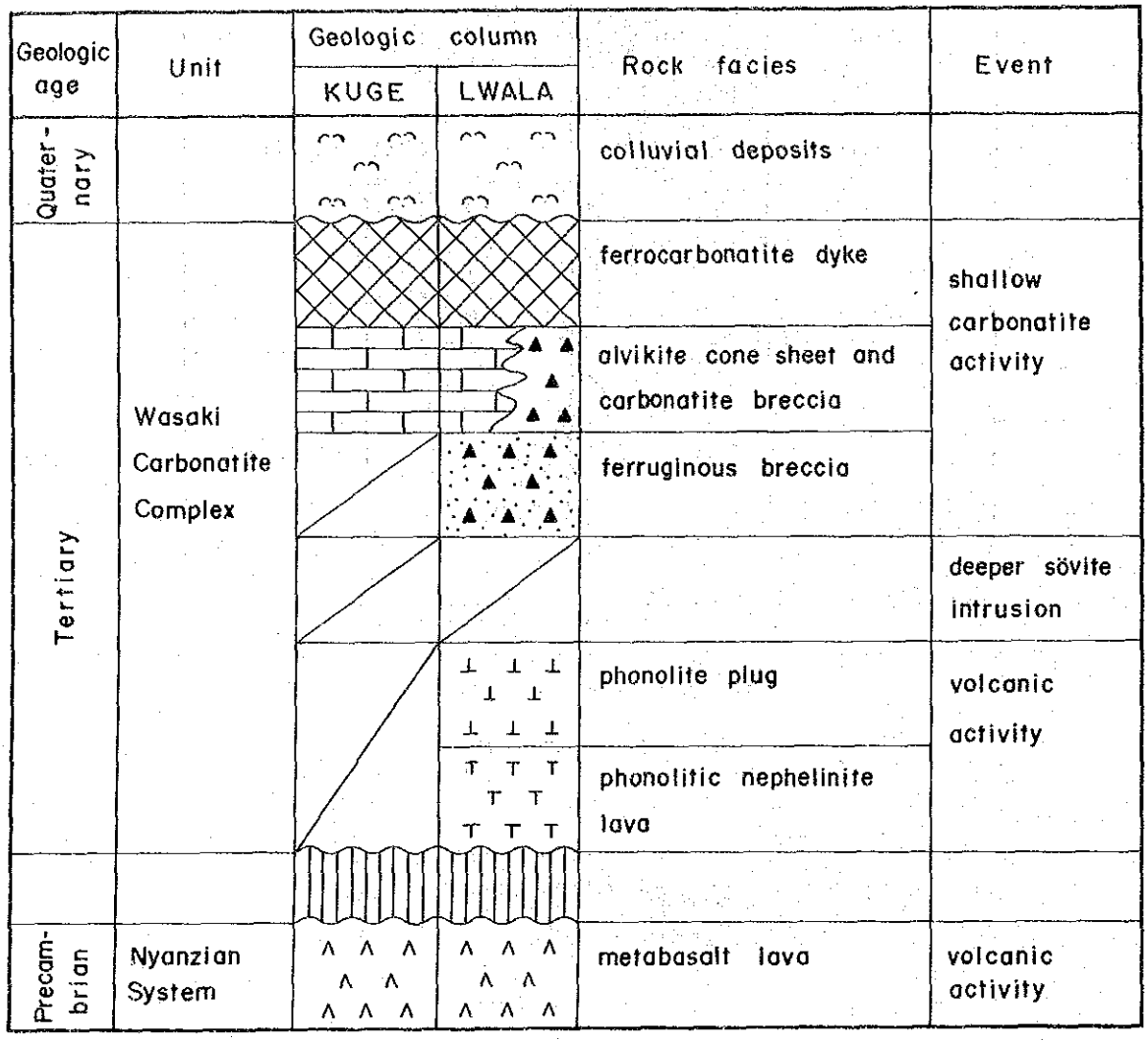

Fig. II – 2 – 2 Generalized Geological Columnar Section of the Kuge–Lwala Area

been fractured (shattered) in the maginal parts which contact ot the outward alvikites.

The rocks of the unit are dark grey to dark greenish grey, fine-grained and compact. Stain by ferric oxide and film-like veinlets of carbonate minerals are common in the rocks.

(2) Alvikite

The unit is distributed in the central part of the sector surrounding the metabasalt mentioned above.

The unit strikes N-S and dips steeply westwards in the west part of the sector, strikes E-S and dips steeply northwards in the north and strikes N-S to NE-SW and dips moderately west to northwestwards in the east, showing circular structure. The southwest part of the sector, on the other hand, shows irregury strikes and dips.

The rocks of the unit show various colours such as pale grey, grey, greyish brown and brown, and are fine to medium-grained banded carbonate rocks comprising mainly carbonate minerals with subordinate mica, magnetitic and apatite. A rock facies which is rich in magnetite sometimes resemble to ferrocarbonatite.

(3) Alvikititic breccia

The unit is distributed in the north part of the sector as a small lenticular body. The body contacts to the northern margine of the alvikite body which forms the main carbonatite facies of the area, suggesting that the unit is brecciated facies of the alvikite body.

The rocks of the unit comprise breccias of alvikite several to several ten centimeters large and small metabasalt, and matrix of greyish brown to reddish grey granular alvikite.

(4) Ferrocarbonatite

The main body of the unit is distributed in the eastern marginal part of the sector trending in N-S direction. The body strikes NNW-SSE to N-S and dips 60° to 80° west. The unit is 60 m maximum wide and 700 m long and comprises a group of several dykes.

There are two small bodies besides the main body, which trend in N-S direction parallel to the alvikites nearby.

The ferrocarbonatites are supposed to be the latest product of carbonatite activity in the sector as they have intruded the alvikites.

The rocks are strongly stained by iron oxide and show such colours as dark brown, dark greyish brown, brown and reddish brown. The rocks are rich in iron and are determined as carbonate rocks because they fumes in reaction to diluted hydrochloric acid.

A sample (Kuge–A) of the ferrocarbonatites collected in the northeastern part of Kuge Hill was microscopically observed and the result is presented in Apx 4 and Apx 10. Microscopically the rock comprises mainly carbonate minerals, barite and goethite with accessary bastnäesite and

mica. EMPA test indicates that the carbonate minerals are calcite, Fe-rich calcite and Fe-Mn rich calcite. Opaque minerals are now entirely composed of goethite.

2–3–2 Lwala Sector

This sector is situated in a rolling plain and there is no circular domed structure which is very common in areas of carbonatite in the Homa Bay Area.

The geology of the sector comprises basement Nyanzian Metabasalt, carbonatitic rocks and phonolitic rocks.

The geological plan and profiles are shown in Fig. II–2–4.

(1) Nyanzian Metabasalt

The unit is distributed in the southwestern, southeastern and northeastern parts of the sector.

The rocks are dark grey to dark greenish grey, altered, fine-grained and compact basaltic rocks and have undergone fracturing. The rocks are stained by iron oxide along fractures and the mafic minerals have changed to ferric iron oxides. The rocks in the southeastern and northeastern part of the sector have altered to pale brown to pinkish brown and brecciated by the intrusion of carbonatites.

(2) Alvikite

The unit is distributed in the central, northeastern and southwestern parts of the area. The structure of the unit is not clear because of scarse outrops.

The rocks are pale grey, brownish grey and pale brown in colour, fine grained, massive partly banded and rich in carbonate minerals with accessary mica and magnetite.

(3) Alvikititic breccia

The unit is distributed in the eastern central part of the sector. The unit is also seen in the east end of the trench dug at the sector.

The rocks are grey to brown carbonatitic breccia comprising breccias of alvikite mentioned above and coarse calcareous matrices.

(4) Ferrocarbonatite

The units are distributed in the northern part of the sector as two small dykes and are also confirmed to exist in the trench as several small dykes, suggesting more occurrences in the sector.

The rocks are brown to dark brown, rich in iron and have been strongly stained by ferric iron oxide. The rocks comprise mainly goethite and carbonate minerals, but sometimes do not produce fumes in reaction to diluted hydrochloric acid because of leaching of carbonate minerals

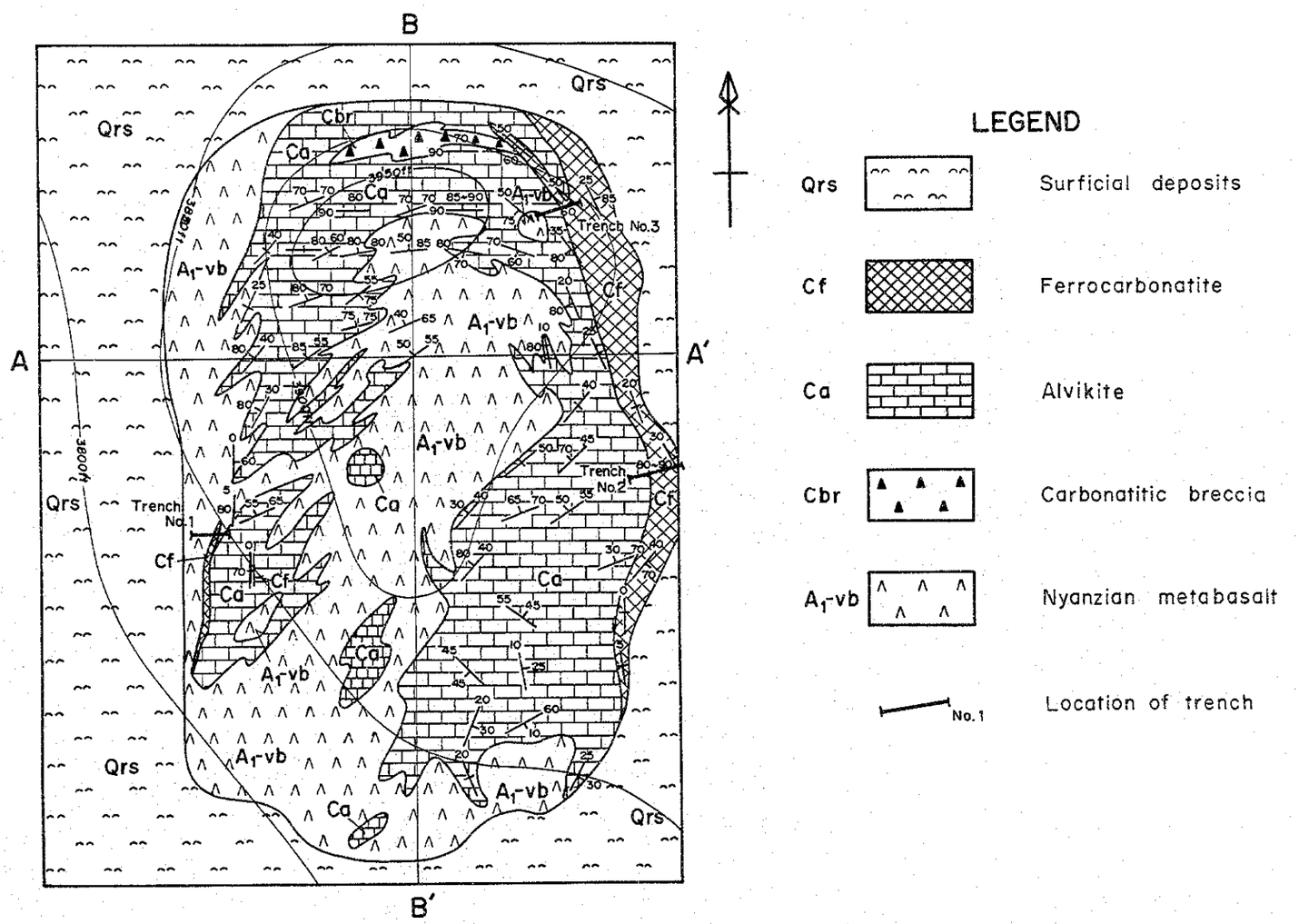

Fig. II – 2 – 3 Geological Map of the Kuge Sector

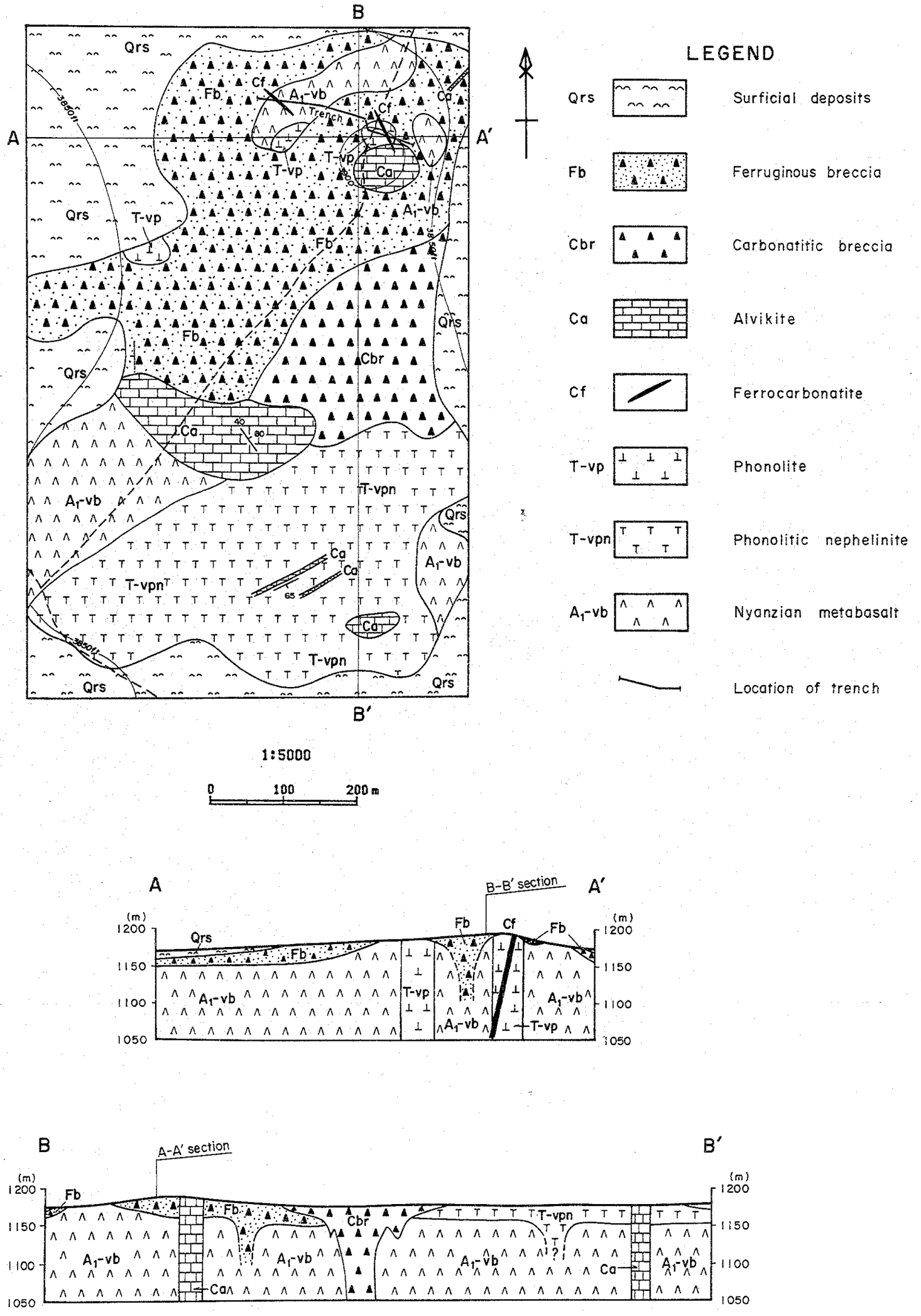

Fig. II – 2 – 4 Geological Map of the Lwala Sector

by weathering.

(5) Ferruginous breccia

The unit is estimated to be widely distributed in the northern part of the sector, but the distribution is not necessarily clear because of the poor outcrops.

The original structure of the rocks is not clear because of strong weathering and contamination by iron oxide. The rocks are generally brown, dark brown and reddish brown, and comprise iron rich matrix and various breccias. Breccias of the rocks are usually less than 2 cm in size and metabasalt, ferrocarbonatite, alvikite and biotite bearing volcanic rocks are the main constituents of the rocks. The amounts and proportions of breccias are variable.

The rocks which occur in the trench located in the northeast part of the sector and the periphery have undergone silicification.

(6) Phonolitic nephelinite

The unit is widely distributed in the southern part of the sector sometimes showing blocky occurrence because of well developed joints.

The rocks are pale grey to grayish green, porphyitic volcanic rocks comprising phenochryst of green prismatic hornblende, prismatic to granular pyroxene, granular nepheline and feldsper replaced by carbonate minerals, and fine crystalline or glassy matrix.

(7) Phonolite

The unit is distributed in the northern part of the sector as three small volcanic necks.

The rocks are pale greenish grey, porphyritic and glassy volcanic rocks comprising phenochrysts of fine nepheline and feldsper and glassy matrix.

2–4 Results of Geochemical Exploration

The survey area comprising two sectors is shwon in Fig. II–2–5 (Phase I results).

2–4–1 Kuge Sector

Seventeen survey lines (A to Q) at 50 m intervals were set in N-S direction and samples were collected in a 50 m interval on each line. Total number of samples is 126 and the sampling points are shown in Apx 49.

(1) Univariate analysis

The summary of statistics of geochemical analysis are shown in Table II–2–1.

In comparison with the summary of "All the Areas" (Table II–3–1), mean values of the elements except γ-ray intensity and U are higher then that of "All the Areas", particularly in L to MREE (La, Ce, Nd, Sm) which have double values of that of "All the Areas". This is due to

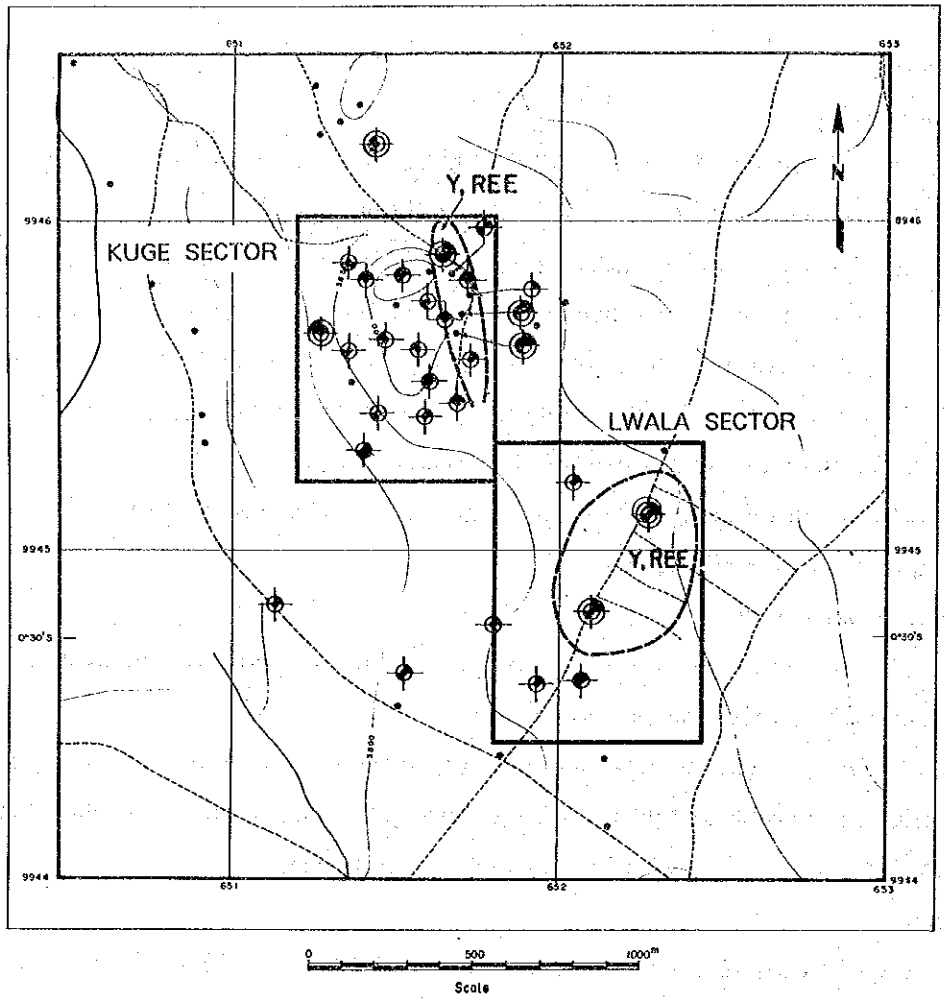

LEGEND

- Non anomalous sample
- Anomalous sample (≧ m+1S , <m+2S)
- Highly anomalous sample (≧ m+2S)
- Geochemicaly anomalous zone (Target area)

Classification

Element	Anomalous, ≧ m+1S, <m+2S	Highly anomalous ≧ m+2S
La ppm	≧ 767 , < 3,300	≧ 3,300
Y ppm	≧ 148 , < 344	≧ 344
Nb ppm	≧ 620 , < 2,600	≧ 2,600
P %	≧ 061 , < 217	≧ 217

m : mean , S : standard deviation

Figures are of 1325 rock samples from all the Semi-detailed Survey Areas other than the grid-sampled areas in the Buru and Ndiru Hills.

Fig. II – 2 – 5 Location Map of Geochemical Survey Area in the Kuge-Lwala Area (Phase I Geochemical Results)

the propotion of samples that metabasalt samples which have low contents in these analytical elements are just 4% in total samples.

(2) Correlation analysis

The correlation coefficients among 16 components including γ-ray intensity are presented in Table II–2–2.

8 elements of REE, Y, Th and BA have mutual coefficients more than 0.5 and the maximum value is 0.976 among Sm and Eu. These 11 elements also correlate positively with γ-ray intensity though the coefficients are variable.

Correlations between these 12 elements and other elements (P, Sr, Nb, U) are less than 0.175 of significant level, and correlation among these 4 elements are also small except that of P-Sr (0.530).

(3) Principal component analysis

Summary of the principal component analysis of major first four components if listed in Table II–2–3.

The cumulative contribution of the major first three components reaches 73%.

The first principal component (Z1) represent 51% of the total amount of information on the analytical data and is thought to be affected by concentration of REE, though the value is very low in comparison with that of other sectors.

The second is strongly affected by P, Sr and Nb, suggesting the wide distribution of alvikite which show higher analytical values in these elements than that of ferrocarbonatite.

The third is affected mainly by U and partly by P and La, indicating the behavior of U.

(4) Geochemically anomalous zones

Cumulative frequency distributions and histgrams of 9 components (P, Nb, Y, Th, La+Ce+Nd, Eu, Yb, γ-ray intensity and score of Z1) are shown in Apx 48, and the density maps with anomalous zones are shown in Apx 50 to 58. Main anomalous zones are summarized as follows.

P, Nb : Anomalous zones are usually distributed in areas of alvikite without overlapping anomalous zones of REE and Y.

Y, Eu, Yb : Major anomalous zones of these elements are distributed in small areas of the southwestern and eastern parts of the sector and rocks of the zones are mostly ferrocarbonatite.

Th : Anomalous zones are distributed in the eastern and western parts of the sector and the zones are almost same as that of Z1.

La+Ce+Nd : Anomalous zones are distributed in the southwestern part and eastern marginal zone of the sector. Almost all rocks include in the zones are ferrocarbonatite.

Table II – 2 – 1 Summary of Statistics of Geochemical Analysis – Kuge Sector –

Component	Unit	Number of sample	Max.	Min.	Mean (M)	Std.dev. (δ)	m+1 δ	m+2 δ	Threshold
γ –ray	cps	126	8005	143	724	0.34	1596	3517	2200
P	%	126	5.640	0.024	0.145	0.47	0.428	1.266	0.630
Ba	ppm	126	24000	790	5040	0.30	10061	20082	
Sr	ppm	126	6790	150	1672	0.31	3380	6833	
Nb	ppm	126	4050	13	405	0.53	1365	4594	1600
Y	ppm	126	670	18	159	0.25	279	491	400
U	ppm	126	80	0.5	1	0.52	5	15	
Th	ppm	126	3383	4	108	0.57	397	1463	460
La	ppm	126	9840	35	850	0.45	2365	6583	
Ce	ppm	126	15950	50	1780	0.39	4401	10881	
Nd	ppm	126	2290	22	640	0.33	1361	2893	
Sm	ppm	126	316.0	3.1	93.7	0.28	179.5	343.8	
Eu	ppm	126	83.2	0.8	26.8	0.27	49.5	91.6	60
Tb	ppm	126	17.7	0.6	6.7	0.25	11.8	20.9	
Yb	ppm	126	26.4	1.4	6.8	0.25	12.1	21.4	18
Lu	ppm	126	5.6	0.3	1.1	0.25	1.9	3.4	
La+Ce+Nd	ppm	126	27500	107	3385	0.38	8083	19304	10000

Remarks : Standard deviation is shown in logarithmic scale.

Table II – 2 – 2 Correlation Coefficient – Kuge Sector –

	γ –ray	P	Ba	Sr	Nb	Y	U	Th	La	Ce	Nd	Sm	Eu	Tb	Yb	Lu
γ –ray																
P	.107															
Ba	.726	.204														
Sr	-.040	.530	.030													
Nb	-.017	.268	.040	.322												
Y	.561	.166	.590	.200	.160											
U	.359	.170	.267	.122	.120	.250										
Th	.860	.130	.787	-.052	-.011	.640	.334									
La	.183	.135	.380	.103	.129	.598	.090	.282								
Ce	.394	.109	.554	.083	.084	.666	.091	.458	.919							
Nd	.580	.115	.713	.097	.139	.782	.141	.679	.686	.859						
Sm	.489	.212	.644	.237	.249	.793	.140	.637	.541	.687	.910					
Eu	.456	.178	.599	.251	.282	.825	.164	.609	.520	.651	.874	.976				
Tb	.350	.157	.470	.259	.238	.860	.134	.470	.482	.559	.731	.857	.898			
Yb	.540	.105	.524	.014	.029	.880	.272	.643	.511	.570	.645	.593	.619	.665		
Lu	.551	.158	.540	.035	.114	.846	.260	.647	.548	.571	.589	.535	.556	.609	.905	

Table II – 2 – 3 Summary of Principal Component Analysis -- Kuge Sector --

Principal Compo.	Eigen Value	Contribution	Cumm. Contribut.	Item	γ-ray	P	Ba	Sr	Nb	Y	U	Th	La	Ce	Nd	Sm	Eu	Tb	Yb	Lu
1	8.221	0.514	0.51	Eigen vector	0.234	0.080	0.265	0.062	0.067	0.324	0.101	0.271	0.234	0.277	0.321	0.312	0.310	0.288	0.287	0.280
				Factor loading	0.671	0.230	0.761	0.176	0.191	0.928	0.290	0.777	0.672	0.794	0.919	0.895	0.890	0.826	0.822	0.802
				Contribution	0.451	0.053	0.579	0.031	0.036	0.862	0.084	0.604	0.451	0.630	0.845	0.802	0.792	0.682	0.675	0.644
2	1.899	0.119	0.63	Eigen vector	-0.309	0.411	-0.174	0.577	0.447	0.021	-0.050	-0.283	0.107	0.027	-0.096	0.131	0.148	0.170	-0.136	-0.111
				Factor loading	-0.426	0.567	-0.240	0.768	0.617	0.028	-0.068	-0.390	0.147	0.037	-0.008	0.181	0.204	0.235	-0.188	-0.153
				Contribution	0.182	0.321	0.058	0.590	0.380	0.001	0.005	0.152	0.022	0.001	0.000	0.033	0.042	0.055	0.035	0.023
3	1.522	0.095	0.73	Eigen vector	0.353	0.385	0.199	0.234	0.124	-0.036	0.492	0.277	-0.372	-0.319	-0.160	-0.084	-0.086	-0.122	0.003	0.042
				Factor loading	0.436	0.475	0.246	0.289	0.153	-0.044	0.607	0.341	-0.459	-0.394	-0.197	-0.104	-0.106	-0.150	0.004	0.052
				Contribution	0.190	0.225	0.060	0.084	0.024	0.002	0.368	0.117	0.211	0.155	0.039	0.011	0.011	0.023	0.000	0.003
4	0.970	0.061	0.79	Eigen vector	-0.153	0.160	-0.219	0.019	-0.086	0.130	0.360	-0.172	0.391	0.174	-0.183	-0.330	-0.301	-0.146	0.339	0.407
				Factor loading	-0.151	0.157	-0.216	0.019	-0.085	0.128	0.355	-0.169	0.386	0.171	-0.180	-0.325	-0.296	-0.144	0.334	0.401
				Contribution	0.023	0.025	0.046	0.000	0.007	0.016	0.126	0.029	0.149	0.029	0.032	0.106	0.088	0.021	0.112	0.161

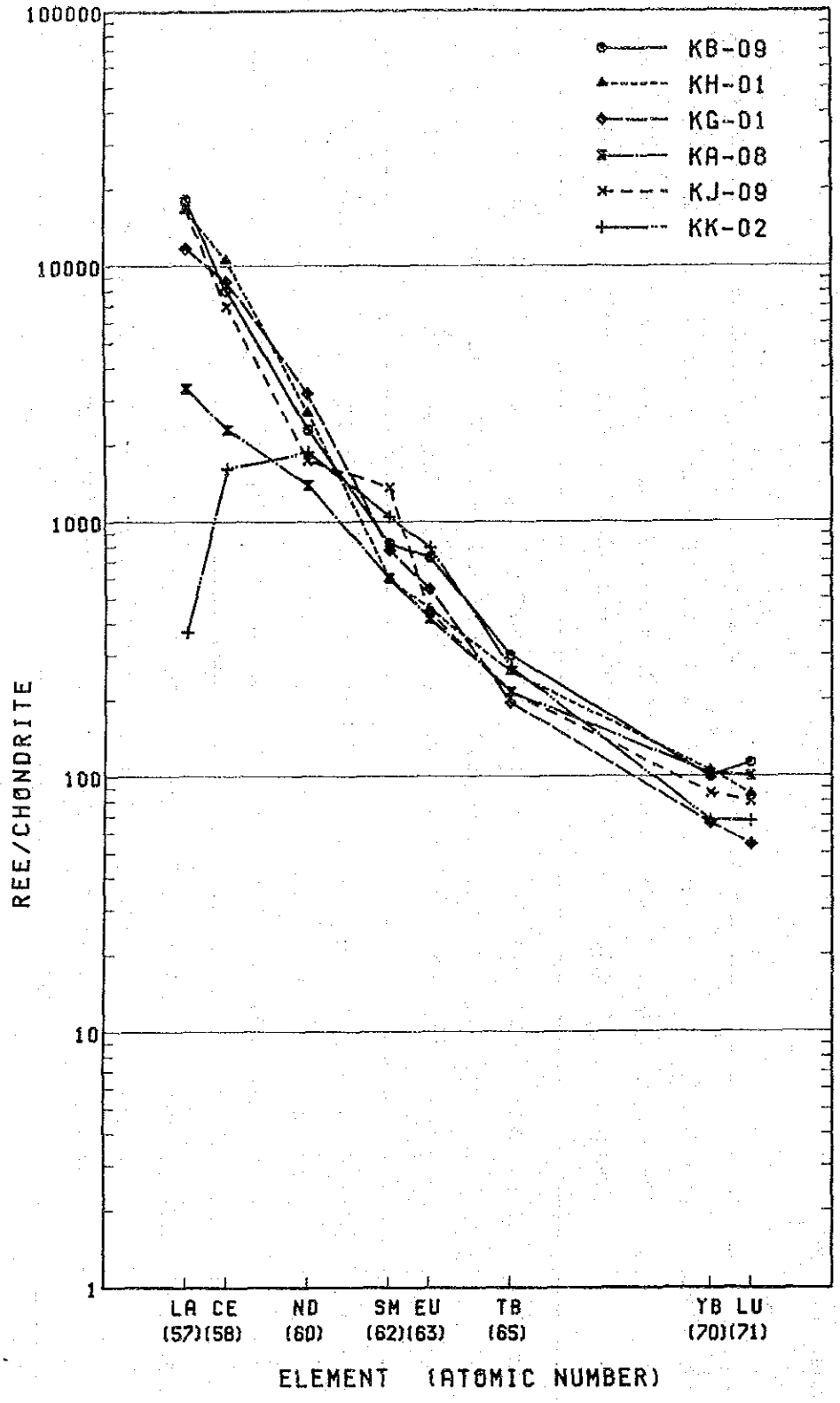

Fig. II – 2 – 6 Chondrite- Normalized REE Patterns, Kuge Sector

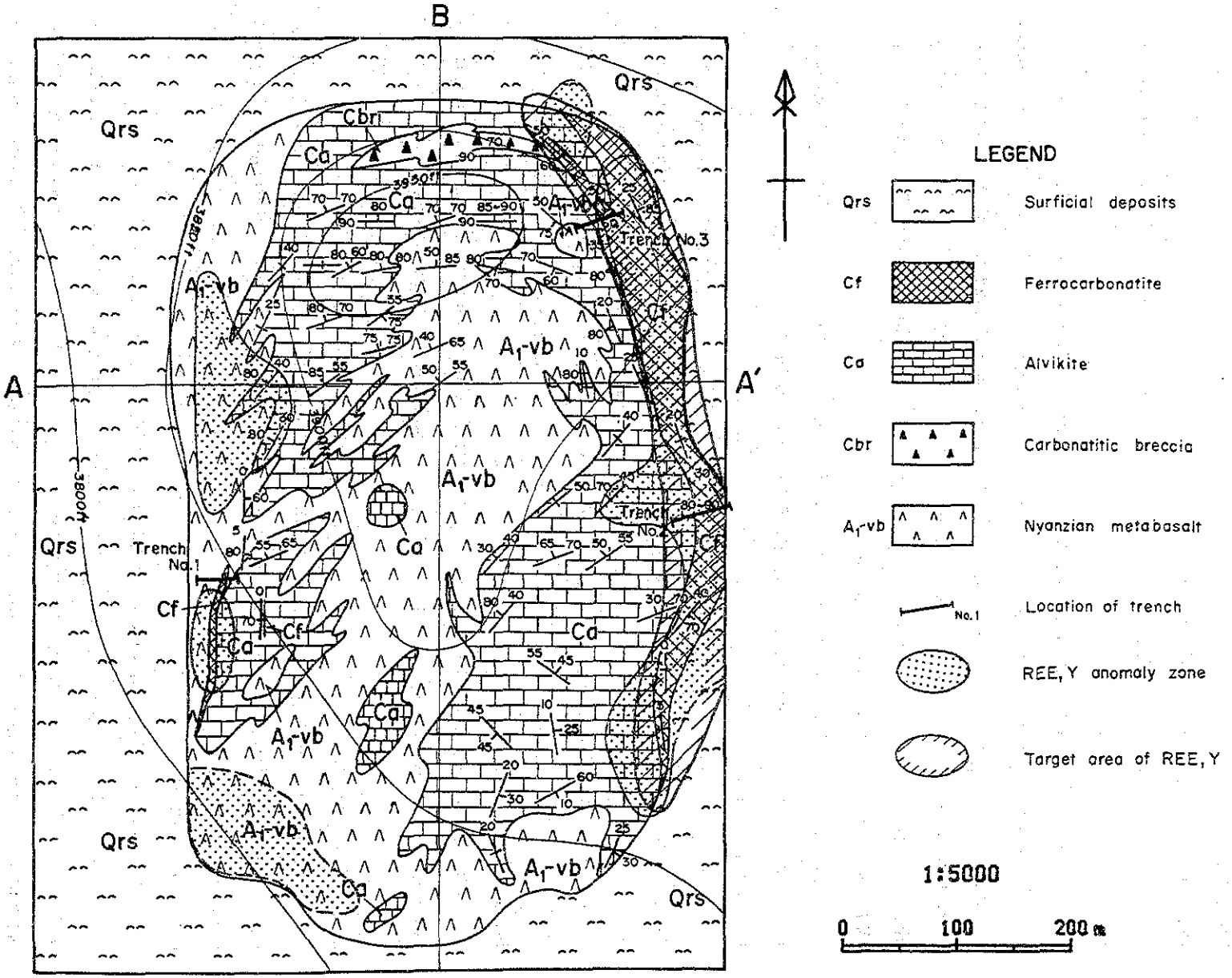

Fig. II – 2 – 7 Geochemical Interpretation Map, Kuge Sector

Z1 : Anomalous zones are widely distributed in both the eastern and western marginal zones of the sector and cover the main parts of anomalous zones of Y, Th, La+Ce+Nd, Eu and Yb which contribute the concentration of REE. Many of rocks included in the zones are ferrocarbonatite.

(5) Chondrite-normalized REE patterns

Six highest score samples of Z1 component are plotted on chondrite-normalized REE patterns (Fig. II–2–6).

Five samples are ferrocarbonatite and the remaining one (KJ–09) is alvikite.

They show normal patterns of carbonatitic rocks except one sample (KK–02) which shows prominent negatite anomaly of Ce and La. Same anomalies as this are also observed in the North Ruri Hill North Sector and the Lwala Sector as described later, and Ohde et. al. (1977) has also mentioned the similar anomaly on samples taken in the Homa Mountain. The alvikite sample (KJ–09) shows remarkable positive anomaly of Sm.

The patterns of ferrocarbonatite by sector (Fig. II–3–3) show that the ferrocarbonatites in the sector are in an average level in contents of REE except Nd.

(6) Interpretation

Through examining geochemical anomalies, it has turned out that 8 elements of REE, Ba, Y, Th and γ-ray intensity are represented by the first component of principal component analysis and the anomalous zones are distributed in two areas ; eastern and southwestern marginal zones of the sector. The anomalous zone of the eastern marginal zone is concordant with the distribution of the ferrocarbonatite dykes, but the southwestern one is situated in a float zone of carbonatite on basement rocks.

The anomalous zone of eastern one is considered to be a potential target area for REE by comprehensive interpretation of the results of both geology and geochemistry (Fig. II–2–7).

2–4–2 Lwala Sector

Nineteen survey lines (A to S) in an interval of 50 m were set in N-S direction and samples were collected at 50 m intervals on leach line. Total number of samples is 140 and the sampling points are shown in Apx 60.

(1) Univariate analysis

The summary of statistics of geochemical analysis are shwon in Table II–2–4.

In comparison with the summary of the "All the Areas", the average values in the sector are higher in Ba, Nb, U, Th, Lu and γ-ray intensity and lower in La and Ce. The maximum values of Nb and Lu of the rocks in the sector are also that of in the "All the Areas". The low mean values

of La and Ce of which are as low as half of that of the "All the Areas" are due to the sample proportions in the sector that ferrocarbonatites and phnolites occupy more than half and 16% of all samples respectively. The ferrocarbonatites in the sector are very poor in La and Ce as it is mentioned later.

(2) Correlation analysis

The correlation coefficients among 16 components including γ-ray intensity are presented in Table II–2–5. The main characters are as the followings.

Eight rare earth elements, Y, Th, Ba and γ-ray intensity mutually correlate positively in coefficents more than 0.5. The maximum coefficent is 0.946 among Sm and Eu.

U correlates positively with other 15 components in coefficients between 0.28 to 0.58 which are higher than the significant level of 5% (0.166), and it differ from the cases of other sectors.

P correlates negatively with Y, Eu, Tb, Yb, Lu and γ-ray intensity.

(3) Principal component analysis

Summary of the principal component analysis of major first four components is listed in Table II–2–6.

The cumulative contribution of the major first three component reaches 81%.

The first principal component (Z1) represents 59% of the total amount of information on the analytical data and is strongly contributed by 8 rare eath elements, Y, Th, Ba and γ-ray intensity, showing the concentration of REE into carbonatites particularly into ferrocarbonatites.

The second is strongly affected by P, Sr and U, and weakly by La.

Nb contributes to the third with a minor affection of Yb and Lu.

(4) Geochemically anomalous zones

Cumulative frequency distributions and histgrams of a components (P, Nb, Y, Th, La+Ce+Nd, Eu, Yb, γ-ray intensity and score of Z1) are shown in Apx 59, and the density maps with anomalous zones are shown in Apx 61 to 69. Main anomalous zones are summarized as the followings.

P, Nb : Anomalous zones of the elements are distributed in the center to the north part of the sector and almost all the rocks in the zones are ferruginous breccias and carbonatites.

Y, Yb: Anomalous zonds and contour patterns of the two elements are very similar and the zones are distributed in the northeastern part of the sector in which rocks are ferruginous breccia and carbonatite.

Th, Eu : Anomalous zones of Th include that of Eu and are distributed in the northeastern and northwestern part of the sector. Major rock type in the zones is ferruginous breccia.

La+Ce+Nd : Anomalous zones are mainly in the northern part and sparsely in the central part of the sector. The forms of the anomalous zones are a little bit different from that of other REE relating components. This is thought to be due to that the ferrocarbontites (ferruginous breccia) in the sector are remarkably low in contents of La and Ce in comparison with ferrocarbonatites in other sectors.

Score of Z1 ; Anomalous zones are distributed in the northeastern and central part of the sector and the zones are similar to that of combined Y, La+Ce+Nd and Eu. The anomalous zones are thought to be represent the hight content zones of REE in the ferruginous breccia zones.

(5) Chondrite-normalized REE patterns

Six highest score samples for Z1 component are plotted on chondrite-normalized REE patterns (Fig. II–2–8). All samples are ferrocarbonatites or ferruginous breccias.

The patterns show big variations in areas of LREE and HREE, but small in an area of MREE. Besides this, the patterns show remarkable characters such as negative anomalies in La and Ce of LK–04, LR–08 and LL–07, a positive anomaly in Lu of LQ–09 and a positive anomaly in Eu of LR–08.

The patterns of ferrocarbonatites by sector (Fig. II–3–3) show that the ferrocarbonatites in the sector are very poor in LREE (La, Ce, Nd) and MREE (Sm, Eu), particularly in La and Ce.

The reasons of low contents and negative anomalies of La and Ce of the ferrocarbonatites (ferruginous breccias) in the sector are not clear, but it is estimated to be due to that the ferruginous breccias are thought to be effusive facies and contain many accidental breccias.

(6) Interpretation

The first principal component (Z1) represents the information of eight rare earth elements, Ba, Y, Th and γ-ray intensityh and as a whole the anomalous zone of the score of Z1 being distributed in the northern part of the sector are thought to represent the concentration of REE. The form of the zone is also very similar to that of combined Y, La+Ce+Nd and Eu. The anomalous zone on the geological map of the sector is shown in Fig. II–2–9.

The ferrocarbonatites/ferruginous breccias have turned out to be poor in REE, paticularly in La and Ce.

2–5 Discussion

2–5–1 Kuge Sector

The geology of the Kuge Hill comprises basement Nyanzian Metabasalt, alvikite and ferrocarbonatite and the carbonatitic rocks show a semicircular structure opened at the southwest.

Table II – 2 – 4 Summary of Statistics of Geochemical Analysis – Lwala Sector –

Component	Unit	Number of sample	Max.	Min.	Mean (M)	Std.dev. (δ)	m+1 δ	m+2 δ	Threshold
γ –ray	cps	140	9608	137	1039	0.39	2572	6368	4000
P	%	140	3.380	0.027	0.129	0.44	0.356	0.984	0.600
Ba	ppm	140	22900	260	3952	0.45	11142	31413	
Sr	ppm	140	6300	113	888	0.39	2166	5282	
Nb	ppm	140	4550	8	208	0.57	774	2882	1000
Y	ppm	140	640	20	124	0.43	332	886	520
U	ppm	140	131	0.5	5	0.52	16	51	
Th	ppm	140	2927	0.5	136	0.84	950	6643	1100
La	ppm	140	6090	5	197	0.58	750	2859	
Ce	ppm	140	11510	7	424	0.62	1784	7502	
Nd	ppm	140	2090	2.5	210	0.66	952	4312	
Sm	ppm	140	372	2.1	39.3	0.61	158.6	639.6	
Eu	ppm	140	99.2	0.25	11.2	0.64	49.1	215.4	69
Tb	ppm	140	22.3	0.1	3.5	0.48	10.5	32.1	
Yb	ppm	140	85.1	0.1	5.5	0.49	16.9	52.5	27
Lu	ppm	140	16.1	0.05	0.9	0.48	2.8	8.4	
La+Ce+Nd	ppm	140	21490	25	903	0.60	3582	14214	5600

Remarks : Standard deviation is shown in logarithmic scale.

Table II – 2 – 5 Correlation Coefficient – Lwala Sector –

	γ –ray	P	Ba	Sr	Nb	Y	U	Th	La	Ce	Nd	Sm	Eu	Tb	Yb	Lu
γ –ray																
P	-.256															
Ba	.776	-.094														
Sr	.036	.445	.262													
Nb	.090	.254	.142	.307												
Y	.766	-.209	.742	.230	.338											
U	.308	.313	.367	.460	.307	.363										
Th	.828	-.052	.819	.215	.183	.765	.417									
La	.431	.190	.565	.515	.369	.580	.584	.606								
Ce	.556	.114	.663	.473	.239	.624	.557	.716	.924							
Nd	.728	.030	.818	.369	.122	.706	.482	.885	.746	.870						
Sm	.820	-.148	.845	.200	.083	.791	.352	.939	.616	.755	.937					
Eu	.836	-.175	.842	.183	.123	.831	.342	.907	.595	.704	.868	.946				
Tb	.811	-.187	.774	.189	.252	.915	.304	.854	.559	.654	.793	.884	.895			
Yb	.654	-.222	.570	.107	.272	.894	.286	.602	.465	.482	.525	.618	.682	.794		
Lu	.596	-.223	.546	.133	.257	.867	.282	.555	.528	.506	.512	.578	.660	.747	.910	

Table II – 2 – 6 Summary of Principal Component Analysis – Lwala Sector –

Prin-cipal Compo.	Eigen Value	Cont-ribu-tion	Cumm. Cont-ribut.	Item	γ-ray	P	Ba	Sr	Nb	Y	U	Th	La	Ce	Nd	Sm	Eu	Tb	Yb	Lu
1	9.414	0.588	0.59	Eigen vector	0.273	-0.027	0.281	0.109	0.090	0.297	0.163	0.298	0.245	0.270	0.297	0.303	0.304	0.302	0.254	0.247
				Factor loading	0.838	-0.084	0.863	0.334	0.277	0.910	0.499	0.914	0.753	0.828	0.910	0.931	0.933	0.926	0.779	0.758
				Contribution	0.703	0.007	0.745	0.112	0.076	0.829	0.249	0.836	0.567	0.686	0.829	0.867	0.871	0.857	0.606	0.575
2	2.315	0.145	0.73	Eigen vector	-0.188	0.522	-0.043	0.475	0.279	-0.112	0.371	-0.036	0.304	0.229	0.082	-0.084	-0.114	-0.130	-0.166	-0.140
				Factor loading	-0.286	0.794	-0.065	0.722	0.425	-0.170	0.564	-0.055	0.463	0.348	0.124	-0.128	-0.174	-0.198	-0.252	-0.213
				Contribution	0.082	0.631	0.004	0.521	0.181	0.029	0.318	0.003	0.214	0.121	0.015	0.016	0.030	0.039	0.064	0.045
3	1.284	0.080	0.81	Eigen vector	-0.101	-0.039	-0.180	0.016	0.563	0.267	0.024	-0.186	0.008	-0.148	-0.283	-0.238	-0.134	0.074	0.412	0.425
				Factor loading	-0.114	-0.044	-0.204	0.018	0.638	0.302	0.027	-0.211	0.009	-0.168	-0.321	-0.269	-0.151	0.084	0.467	0.482
				Contribution	0.013	0.002	0.041	0.000	0.408	0.091	0.001	0.044	0.000	0.028	0.103	0.072	0.023	0.007	0.218	0.232
4	0.654	0.041	0.85	Eigen vector	0.188	0.348	0.181	-0.161	0.564	-0.010	-0.215	0.255	-0.325	-0.280	0.002	0.114	0.109	0.141	-0.166	-0.313
				Factor loading	0.152	0.281	0.147	-0.130	0.456	-0.008	-0.174	0.206	-0.263	-0.226	0.002	0.092	0.088	0.114	-0.136	-0.253
				Contribution	0.023	0.079	0.022	0.017	0.208	0.000	0.030	0.042	0.069	0.051	0.000	0.008	0.008	0.013	0.018	0.064

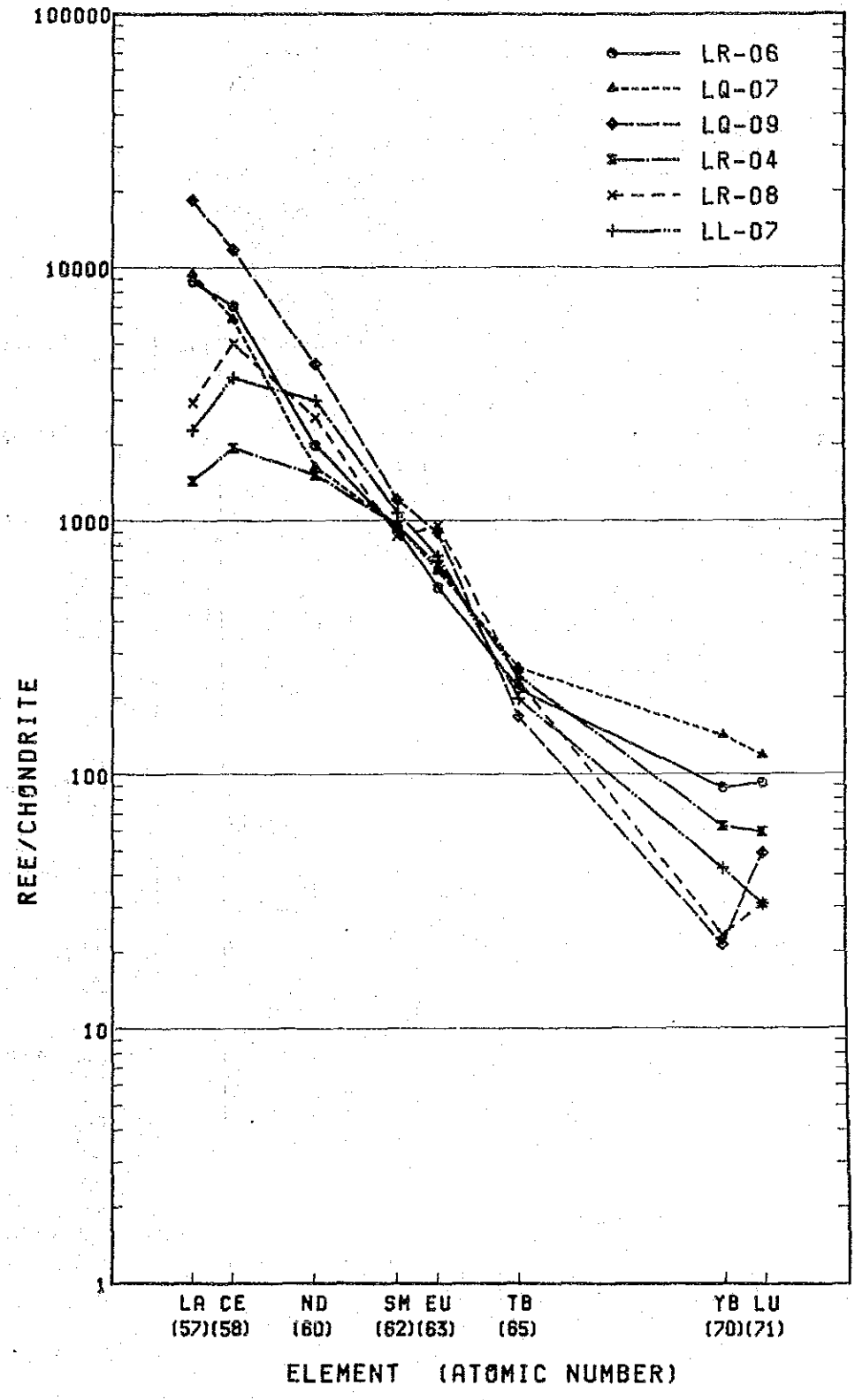

Fig. II – 2 – 8 Chondrite- Normalized REE Patterns, Lwala Sector

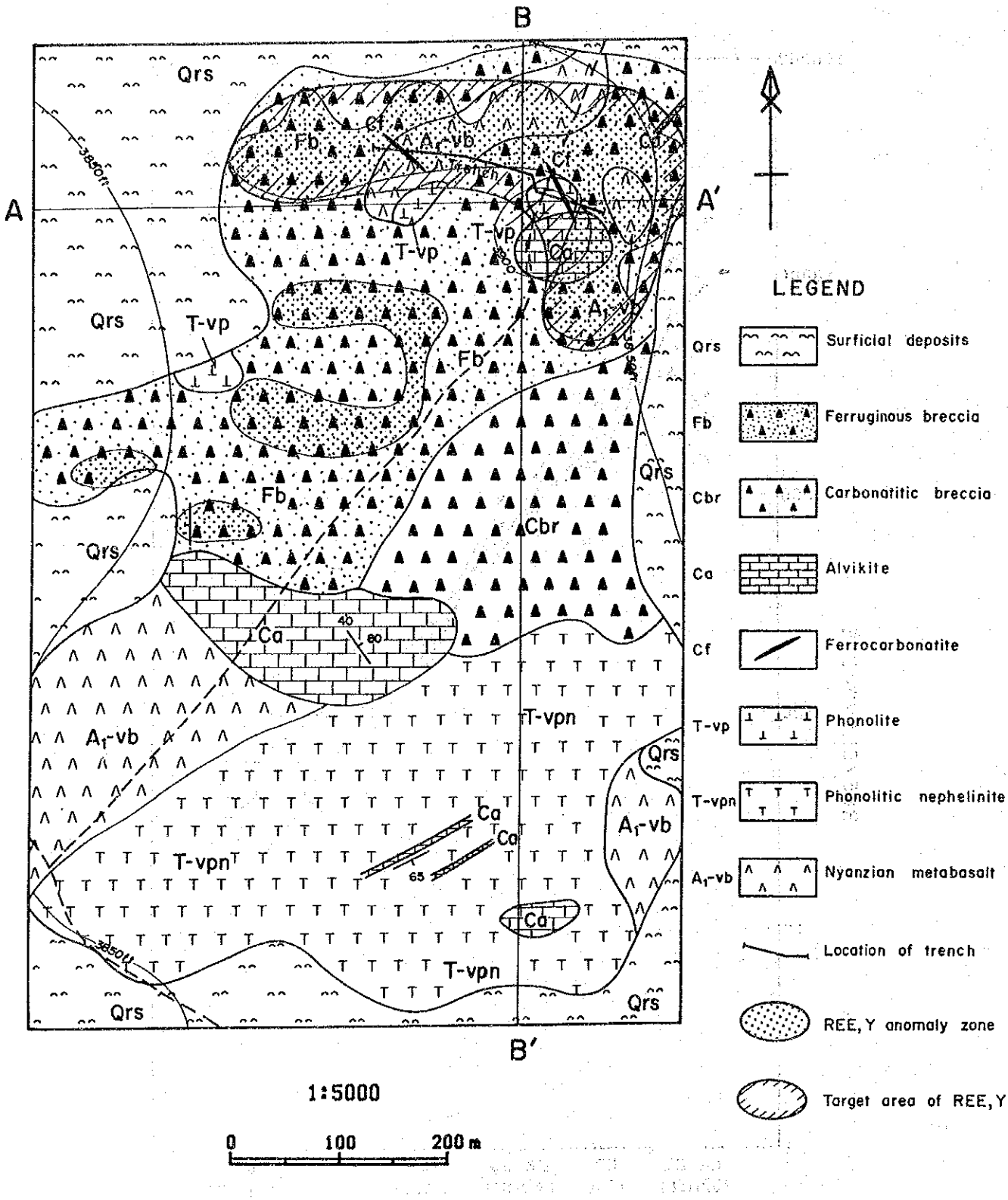

Fig. II – 2 – 9 Geochemical Interpretation Map, Lwala Sector

Major body of ferrocarbonatites is distributed in the eastern marginal part of the sector as a group of dykes, 60 m in maximum width ad 700 m in length. They strike N-S direction and dip 60° to 80° west or vertically. Besides this body there are two small ferrocarbonatite dykes in the southwestern part of the sector.

Geochemically anomalous zones of the scores of the first principal component in the principal component analysis which represent the major anomalous zones of Y, Th, La + Ce + Nd, Eu and Yb as a whole are distributed in the eastern and southwestern marginal part of the sector.

The area of the former overlies the major ferrocarbonatite dykes, but the later are situated in the float zone of carbonatite on basement rocks.

The ferrocarbonatites in the sector have average patterns on chondrite-normalized patterns by sector except high content of Nd.

The anomalous zone in the eastern nmarginal part of the sector is thought ot be a potential target area for REE and Y.

2–5–2 Lwala Sector

The geology of the sector comprises basement Nyanzian Metabasalt, carbonatitc rocks and phonolitic rocks. The felluginous breccias which were thought to be a potential target area for REE from the results of Phase I have turned out to be effusive facies of carbonatite. It comprises various breccias such as ferrocarbonatite, alvikite and metabasalt, and ferruginous matrix.

Major geochemically anomalous zones are distributed in the northern part of the sector, of which are that of Y, La + Ce + Nd and Eu, and are represented by the anomalous zone of score of Z1. The zone is small in scale.

Chondrite-normalized REE patterns show the low contents of REE, particularly of LREE in the ferrocarbonatites in the sector.

The anomalous zone covering the ferruginous breccias in the northern part of the sector is considered to be worthless for further follow-up explorations in Phase III.

CHAPTER 3 GENERAL DISCUSSION ON THE GEOCHEMICAL EXPLORATIONS

3–1 Results of Geochemical Explorations

Results of univariate statistical analysis, correlation analysis and principal component analysis for analytical results of 16 component (15 element and γ-ray intensity) of all samples (590) in all survey sectors are shown in Table II–3–1, II–3–2 and II–3–3 respectively. Considering the results of principal component analysis of this year (refer II–1–4 and II–2–4) and the results of Phase I, presentation of cumulative frequency distributions and histograms of elements, threshold analysis, geochemical density and anomaly maps were limited to 9 components of P, Nb, Y, Th, La+Ce+Nd, Eu, Yb γ-ray intensity and scores of Z1 of principal component analysis.

Thresholds were decided by using the method of Otsu et. al. (1983).

3–1–1 Univariate analysis

Results by sector have been mentioned in II–1–4 and II–2–4. The average values of each elements depend on proportion of rock types in a group samples, then the comparison of average values of elements by sector is not so significant. The proportions of rock types of each sector are shown below.

Propotions of Rock Types

Area	Rock Type	FCB	ALV	SOV	CBB	PHN	MTBT	Total
KUGE	No.	22	99	0	0	0	5	126
	%	17	79	0	0	0	4	100
LWALA	No.	75	24	0	9	22	10	140
	%	54	17	0	6	0	7	100
NRHN	No.	20	52	2	6	0	1	81
	%	25	64	2	7	0	1	100
NRHS	No.	29	109	5	2	0	5	150
	%	19	73	3	1	0	3	100
SRH	No.	37	15	0	2	0	39	93
	%	40	16	0	2	0	42	100
Total	No.	183	299	7	19	22	60	590
	%	31	51	1	3	4	10	100

Abbreviations (Name of Sector)

KUGE : Kuge Sector in the Kuge-Lwala Area
LWALA: Lwala Sector in the Kuge-Lwala Area
NRHN : North Ruri Hill North sector in the North & South Ruri Hill Area
NRHS : North Ruri Hill South Sector in the North & South Ruri Hill Area
SRH : South Ruri Hill Sector in the North & South Ruru Hill Area

Abbreviations (Rock)

FCB : Ferrocarbonatite, Ferruginous breccia
ALV : Alvikite
SOV : Sövite
CBB : Carbonatitic breccia
PHN : Phonolite
MTBT : Metabasalt

Summary of statistics by rock type classified as above are shown in Table II–3–4 to II–3–9. From the tables following characters among 6 rock types are noticed.

FCB > ALV, CBB, SOV > PHN, MTBT in REE, Y and γ-ray intensity
FCB > ALV > CBB > SOV > PHN > MTBT in La, Ce, Nd, Sm, Eu and Tb
FCB > CBB > ALV > PHN > SOV > MTBT in Ba and Tb

These relations show concentration of REE, Y and Ba in carbonatitic rocks, particularly in ferrocarbonatite.

Following characters are also observed in U, Nb, Sr and P.

FCB > CBB > PHN > ALV > SOV > MTBT in U
CBB > PHN > ALV > FCB > SOV > MTBT in Nb
SOV > ALV > CBB > PHN > FCB > MTBT in Sr
SOV > PHN > ALV > CBB > FCB > MTBT in P

Conspicuous characters are low contents of Nb, Sr and P, in FCB and high contents of Sr and P in SOV.

These characters by rock type are also seen in the results of principal component analysis for all samples, that is, REE, Ba, Y, Th and γ-ray intensity contribute strongly to the first principal component, and the remaining 4 elements (U, Nb, Sr, P) to the second to fifth principal components.

3–1–2 Correlation analysis

The correlation coefficients among 9 elements ; Ba,Y, Th, La, Ce, Nd, Sm, Eu and Tb are

higher than 0.64 and the highest coefficients is 0.977 among Sm and Eu. The correlation coefficients of Yb, Lu and γ-ray intensity with the 9 elements are also high (0.47 to 0.89), indicating mutual positive correlation among these 12 elements.

Correlation coefficients of P, Sr, Nb and U with the 12 elements are very low (0.2 to 0.4) though the coefficients are higher than the significant level of 5% (0.08).

3–1–3 Principal component analysis

Contributions of 12 elements (Ba, Y, Th, La, Ce, Nd, Sm, Eu, Tb, Yb, Lu and γ-ray intensity) to the first principal component (Z1) reache 63% and the component seems to be related with carbonatite, especially with the distribution of ferrocarbonatite.

The second principal component is strongly affected by Sr and P, and the component is thought to represent the distribution mainly of carbonatite, especially sövite and alvikite, and partly of phonolite.

The third is affected by U and this means that U behaves independently of other elements.

The fourth, though the contribution to all the information is low, is affected by Yb and Lu, suggesting a different process of concentration of HREE from LREE and MREE.

3–1–4 Chondrite-normalized REE patterns

Chondrite-normalized REE patterns of all rocks by survey sector, by rock type in all survey sectors and of ferrocarbonatite by survey sector are shown in Fig. II–3–1, Fig. II–3–2 and Fig. II–3–3 respectively.

Simple comparison of contents of REE by sector shows the descending order, from KUGE to NRHN, NRHS, LWALA and SRH. But the significance is not hight because the proportions of samples in each sector are different.

Fig. II–3–3 indicate the following characters of ferrocarbonatites by sector.

La, Ce : NRHS > SRH, KUGE > NRHN ≫ LWALA

Nd, Sm: KUGE > SRH > NRHN > NRHS > LWALA

Eu : NRHN > SRH > KUGE > NRHS > LWALA

Tb, Yb, Lu : NRHN > NRHS > KUGE > LWALA > SRH

Fig. II–3–2 shows following characters of each rock type in REE concentration.

Abundances of REE : FCB > ALV > CBB > SOV > PHN > MTBT.

Carbonatitic rocks ; FCB, ALV, CBB and SOV show similar patterns ascending to a LREE side from a HREE side.

PHN shows also a similar pattern to carbonatitic rocks though it shows negative Eu anomaly

which might mean much differentiation from magma than carbonatitic rocks.

MTBT shows a different pattern to other rock types and the pattern suggest smaller differentiation from magma than others.

3–2 Discussion

Geochemical characters and exploration potentials for each sector are summarized as followings.

3–2–1 North Ruri Hill North Sector

A major geochemically anomalous zone is in the northern part of the sector where ferrocarbonatite breccias and ferrocarbonatite dykes occur. The zone is represented by the anomaly zone of score of the first principal component (Z1) in principal component analysis.

The ferrocarbonatite breccias and dykes are rich in HREE (Tb, Yb, Lu) in comparison with that of other sectors.

The anomalous zone may be a main target area of REE in the sector but the potential is thought to be low because of the small size of the area (0.03 km^2) and heterogeneous character of the rocks in contents of REE.

3–2–2 North Ruri Hill South Sector

A major geochemically anomalous zone is in the south part of the sector where dyke swarms of small ferrocarbonatite occur. The anomalous zone is represented by that of score of Z1 which includes anomalous zones of REE, Ba, Y, Th and γ-ray intensity.

Ferrocarbonatites in the zone are rich in La and Ce in comparison with that of other sectors.

But the zone is considered to be not a potential target area for REE because of the small dyke character of ferrocarbonatites, though they show some high contents in La and Ce.

3–2–3 South Ruri Hill Sector

A major geochemically anomalous zone represented by anomalous zones of score of Z1 and La+Ce+Nd is in the central to northern part of the sector. The zone covers an area of dyke swarms of ferrocarbonatite. The dyke swarms comprise a group of small ferrocarbonatite dykes which are usually less than 0.5 m wide and several tens of meters long. The ferrocarbonatites are rich in La and Ce but poor in Yb and Lu in comparison with that of other sectors.

It is considered that no further follow-up is necessary for the zone, as the ferrocarbonatite dykes are too small to form a single unit big enough for follow-up explorations.

3–2–4 Kuge Sector

Major geochemically anomalous zones are in two areas, eastern and southwestern marginal parts of the sector.

The former area covers a zone of ferrocarbonatite 60 m maximum wide and 700 m long, and the later one covers a float zone of carbonatite on basement rocks.

The ferrocarbonatites in the anomalous zone of eastern marginal part of the sector show a character rich in Nd in comparison with that of other sectors.

The eastern anomalous zone is considered to be a potential target area of REE and Y, for Phase III by comprehensive interpretation of Phase II and Phase I results.

3–2–5 Lwala Sector

There is a major geochemically anomalous zone in the northern part of the sector. The anomalous zone is represented by that of the scores of Z1 in principal component analysis, which summarizes all anomalies of REE, Ba, Y, Th and γ-ray intensity found in the sector.

The anomalous zone is in a zone of thin ferruginous breccias which are thought to be a effusive facies of carbonatite.

The ferruginous breccias have a character poor in REE, particularly in La and Ce in comparison with that of other sectors.

Because of the low contents of REE and the small thickness of the ferruginous breccias, the zone is considered to be not a potential target area of REE for Phase III.

Table II – 3 – 1 Summary of Statistics of Geochemical Analysis – All Geochemical Areas –

Component	Unit	Number of sample	Max.	Min.	Mean (M)	Std.dev. (δ)	m+1 δ	m+2 δ	Threshold
γ –ray	cps	590	9608	75	816	0.39	2004	4918	6400
P	%	590	5.640	0.014	0.144	0.51	0.462	1.488	0.630
Ba	ppm	590	36100	170	3122	0.49	9654	29858	
Sr	ppm	590	12180	92	1341	0.46	3890	11284	
Nb	ppm	590	4550	2.5	152	0.72	794	4142	1090
Y	ppm	590	2300	13	128	0.42	338	891	400
U	ppm	590	247	0.5	3	0.60	13	50	
Th	ppm	590	3383	0.5	76	0.82	500	3315	1170
La	ppm	590	14330	3	422	0.71	2182	11286	
Ce	ppm	590	19470	7	835	0.71	4234	21473	
Nd	ppm	590	5500	2.5	290	0.67	1346	6255	
Sm	ppm	590	826	1.5	49.4	0.57	183.3	679.9	
Eu	ppm	590	233	0.25	14.7	0.57	54.1	199.1	130
Tb	ppm	590	60.2	0.1	4.1	0.50	13.1	41.3	
Yb	ppm	590	113.0	0.1	5.8	0.41	15.1	39.1	60
Lu	ppm	590	16.1	0.05	1.0	0.39	2.3	5.8	
La+Ce+Nd	ppm	590	36640	14	1624	0.69	7894	38380	7500

Remarks : Standard deviation is shown in logarithmic scale.

Table II – 3 – 2 Correlation Coefficient – All Geochemical Areas –

	γ –ray	P	Ba	Sr	Nb	Y	U	Th	La	Ce	Nd	Sm	Eu	Tb	Yb	Lu
γ –ray																
P	.171															
Ba	.749	.192														
Sr	.251	.603	.306													
Nb	.315	.384	.412	.446												
Y	.733	.262	.761	.433	.424											
U	.417	.340	.321	.306	.304	.349										
Th	.815	.169	.813	.273	.349	.801	.362									
La	.478	.347	.644	.509	.415	.726	.326	.648								
Ce	.564	.324	.709	.586	.406	.754	.328	.718	.970							
Nd	.674	.274	.798	.519	.414	.792	.310	.815	.857	.928						
Sm	.690	.228	.796	.463	.397	.828	.275	.843	.804	.878	.962					
Eu	.703	.222	.790	.460	.401	.856	.290	.833	.789	.855	.931	.977				
Tb	.682	.274	.748	.493	.454	.903	.295	.790	.765	.813	.863	.912	.927			
Yb	.620	.193	.603	.299	.302	.896	.283	.674	.584	.594	.602	.651	.696	.764		
Lu	.586	.153	.600	.241	.284	.866	.272	.655	.591	.590	.584	.631	.676	.726	.930	

Table II – 3 – 3 Summary of Principal Component Analysis – All Geochemical Areas –

Principal Compo.	Eigen Value	Contribution	Cumm. Contribut.	Item	γ-ray	P	Ba	Sr	Nb	Y	U	Th	La	Ce	Nd	Sm	Eu	Tb	Yb	Lu
1	10.062	0.629	0.63	Eigen vector	0.243	0.109	0.266	0.171	0.158	0.294	0.131	0.275	0.270	0.283	0.294	0.296	0.298	0.295	0.251	0.244
				Factor loading	0.772	0.347	0.843	0.544	0.500	0.931	0.417	0.873	0.855	0.899	0.932	0.939	0.944	0.937	0.795	0.773
				Contribution	0.595	0.120	0.710	0.296	0.250	0.867	0.173	0.762	0.732	0.808	0.868	0.882	0.891	0.878	0.632	0.598
2	1.682	0.105	0.73	Eigen vector	-0.171	0.574	-0.119	0.524	0.336	-0.114	0.242	-0.179	0.151	0.107	0.016	-0.058	-0.074	-0.045	-0.198	-0.226
				Factor loading	-0.221	0.745	-0.155	0.679	0.436	-0.147	0.314	-0.232	0.196	0.139	0.020	-0.075	-0.096	-0.059	-0.257	-0.293
				Contribution	0.049	0.555	0.024	0.462	0.190	0.022	0.098	0.054	0.038	0.019	0.000	0.006	0.009	0.003	0.066	0.086
3	1.044	0.065	0.80	Eigen vector	0.272	0.200	0.014	-0.137	0.162	0.142	0.593	0.065	-0.270	-0.288	-0.259	-0.228	-0.171	-0.069	0.284	0.274
				Factor loading	0.277	0.204	0.015	-0.140	0.165	0.145	0.606	0.066	-0.276	-0.294	-0.264	-0.233	-0.175	-0.071	0.290	0.280
				Contribution	0.077	0.042	0.000	0.020	0.027	0.021	0.367	0.004	0.076	0.086	0.070	0.054	0.031	0.005	0.084	0.078
4	0.852	0.053	0.85	Eigen vector	-0.321	0.169	-0.271	0.181	-0.049	0.219	-0.410	-0.249	0.069	-0.027	-0.162	-0.116	-0.061	0.095	0.459	0.461
				Factor loading	-0.296	0.156	-0.251	0.167	-0.045	0.202	-0.378	-0.230	0.063	-0.025	-0.149	-0.107	-0.056	0.088	0.424	0.425
				Contribution	0.088	0.024	0.063	0.028	0.002	0.041	0.143	0.053	0.004	0.001	0.022	0.011	0.003	0.008	0.180	0.181

Table II – 3 – 4 Summary of Statistics of Geochemical Analysis by Rock Type – Ferrocarbonatite –

Component	Unit	Number of sample	Max.	Min.	Mean (M)	Std.dev. (δ)	m+1 δ	m+2 δ	Threshold
γ –ray	cps	183	9608	398	1880	0.29	3656	7110	
P	%	183	3.380	0.022	0.126	0.43	0.343	0.931	
Ba	ppm	183	36100	540	7916	0.29	15258	29411	
Sr	ppm	183	6970	184	1132	0.36	2599	5971	
Nb	ppm	183	4550	2.5	159	0.62	666	2789	
Y	ppm	183	2300	40	258	0.33	553	1185	
U	ppm	183	131	0.5	5	0.52	17	55	
Th	ppm	183	3383	9	420	0.53	1408	4723	
La	ppm	183	12100	26	756	0.63	3254	13998	
Ce	ppm	183	19430	20	1742	0.59	6775	26359	
Nd	ppm	183	5500	25	751	0.49	2294	7012	
Sm	ppm	183	826	5.5	119.3	0.42	310.9	810.2	
Eu	ppm	183	233	1.8	35.3	0.38	84.4	202.1	
Tb	ppm	183	60.2	0.6	8.4	0.33	17.8	37.6	
Yb	ppm	183	113.0	0.1	10.8	0.37	25.2	59.0	
Lu	ppm	183	16.1	0.2	1.7	0.32	3.6	7.5	
La+Ce+Nd	ppm	183	34270	90	3605	0.53	12117	40732	

Remarks : Standard deviation is shown in logarithmic scale.

Table II – 3 – 5 Summary of Statistics of Geochemical Analysis by Rock Type – Alvikite –

Component	Unit	Number of sample	Max.	Min.	Mean (M)	Std.dev. (δ)	m+1 δ	m+2 δ	Threshold
γ –ray	cps	299	4407	254	700	0.22	1167	1951	
P	%	299	5.640	0.014	0.197	0.48	0.590	1.771	
Ba	ppm	299	21400	310	2843	0.35	6375	14294	
Sr	ppm	299	12180	231	2242	0.29	4356	8466	
Nb	ppm	299	4050	2.5	240	0.58	914	3486	
Y	ppm	299	1300	13	132	0.27	243	447	
U	ppm	299	247	0.5	3	0.61	13	55	
Th	ppm	299	1311	2	60	0.47	176	520	
La	ppm	299	14330	23	652	0.41	1680	4329	
Ce	ppm	299	19470	33	1212	0.39	2967	7265	
Nd	ppm	299	3910	6	362	0.37	843	1965	
Sm	ppm	299	316	2.9	57.4	0.33	121.7	258.0	
Eu	ppm	299	80.2	1.1	17.3	0.31	35.6	73.3	
Tb	ppm	299	31.9	0.5	4.8	0.30	9.5	18.9	
Yb	ppm	299	76.0	0.4	5.7	0.31	11.6	23.6	
Lu	ppm	299	11.8	0.05	0.9	0.30	1.8	3.7	
La+Ce+Nd	ppm	299	36640	62	2259	0.39	5516	13472	

Remarks : Standard deviation is shown in logarithmic scale.

Table II – 3 – 6 Summary of Statistics of Geochemical Analysis by Rock Type – Sövite –

Component	Unit	Number of sample	Max.	Min.	Mean (M)	Std.dev. (δ)	m+1 δ	m+2 δ	Threshold
γ –ray	cps	7	859	293	427	0.15	600	843	
P	%	7	1.150	0.246	0.534	0.25	0.942	1.661	
Ba	ppm	7	2410	410	866	0.24	1509	2630	
Sr	ppm	7	8020	3820	6213	0.12	8262	10985	
Nb	ppm	7	98	10	33	0.33	70	149	
Y	ppm	7	71	46	56	0.06	64	73	
U	ppm	7	25	0.5	2	0.59	9	36	
Th	ppm	7	30	5	8	0.25	14	26	
La	ppm	7	242	185	223	0.04	244	267	
Ce	ppm	7	576	362	446	0.07	521	609	
Nd	ppm	7	167	90	122	0.08	146	175	
Sm	ppm	7	27.7	16.7	21.7	0.07	25.4	29.7	
Eu	ppm	7	11.1	5.3	6.8	0.11	8.8	11.4	
Tb	ppm	7	3.6	1.5	2.0	0.11	2.5	3.2	
Yb	ppm	7	5.2	2.4	3.5	0.11	4.5	5.8	
Lu	ppm	7	0.9	0.3	0.5	0.13	0.7	1.0	
La+Ce+Nd	ppm	7	983	657	793	0.06	904	1031	

Remarks : Standard deviation is shown in logarithmic scale.

Table II – 3 – 7 Summary of Statistics of Geochemical Analysis by Rock Type – Carbonatite Pyroclastics –

Component	Unit	Number of sample	Max.	Min.	Mean (M)	Std.dev. (δ)	m+1 δ	m+2 δ	Threshold
γ –ray	cps	22	495	254	371	0.08	446	536	
P	%	22	0.403	0.299	0.362	0.03	0.391	0.422	
Ba	ppm	22	19250	630	1460	0.35	3233	7157	
Sr	ppm	22	2200	725	1201	0.13	1599	2131	
Nb	ppm	22	400	80	332	0.19	515	798	
Y	ppm	22	39	25	32	0.05	36	40	
U	ppm	22	10	0.5	4	0.39	10	24	
Th	ppm	22	37	7	27	0.19	41	62	
La	ppm	22	102	66	74	0.05	82	92	
Ce	ppm	22	186	104	144	0.07	168	196	
Nd	ppm	22	77	45	60	0.06	68	77	
Sm	ppm	22	10.4	8.3	9.2	0.03	9.8	10.5	
Eu	ppm	22	4.3	0.25	1.8	0.38	4.4	10.7	
Tb	ppm	22	1.2	0.6	0.9	0.07	1.0	1.2	
Yb	ppm	22	2.8	0.1	1.0	0.29	2.1	4.0	
Lu	ppm	22	0.4	0.05	0.1	0.29	0.3	0.5	
La+Ce+Nd	ppm	22	354	225	278	0.05	312	349	

Remarks : Standard deviation is shown in logarithmic scale.

Table II – 3 – 8 Summary of Statistics of Geochemical Analysis by Rock Type – Phonolite –

Component	Unit	Number of sample	Max.	Min.	Mean (M)	Std.dev. (δ)	m+1 δ	m+2 δ	Threshold
γ –ray	cps	19	4011	301	1049	0.25	1863	3307	
P	%	19	0.715	0.036	0.137	0.38	0.329	0.793	
Ba	ppm	19	10460	1710	3819	0.21	6174	9982	
Sr	ppm	19	6300	200	1084	0.35	2422	5414	
Nb	ppm	19	1450	100	402	0.30	801	1596	
Y	ppm	19	510	38	152	0.34	331	720	
U	ppm	19	64	0.5	4	0.50	13	41	
Th	ppm	19	347	23	91	0.34	197	425	
La	ppm	19	1845	59	306	0.43	828	2243	
Ce	ppm	19	2360	110	528	0.43	1403	3731	
Nd	ppm	19	646	41	192	0.35	427	947	
Sm	ppm	19	96.1	7.5	32.3	0.34	71.0	155.8	
Eu	ppm	19	20.6	2.6	10.7	0.33	22.6	48.0	
Tb	ppm	19	10.4	0.8	3.6	0.33	7.7	16.4	
Yb	ppm	19	26.4	0.8	7.8	0.38	18.6	44.3	
Lu	ppm	19	3.7	0.3	1.3	0.32	2.7	5.6	
La+Ce+Nd	ppm	19	4851	218	1045	0.40	2638	6659	

Remarks : Standard deviation is shown in logarithmic scale.

Table II – 3 – 9 Summary of Statistics of Geochemical Analysis by Rock Type – Metabasalt –

Component	Unit	Number of sample	Max.	Min.	Mean (M)	Std.dev. (δ)	m+1 δ	m+2 δ	Threshold
γ –ray	cps	60	1002	75	184	0.27	339	627	
P	%	60	0.350	0.014	0.028	0.24	0.048	0.085	
Ba	ppm	60	3560	170	419	0.31	849	1719	
Sr	ppm	60	2470	92	162	0.29	312	601	
Nb	ppm	60	670	2.5	9	0.56	33	118	
Y	ppm	60	175	16	23	0.18	35	53	
U	ppm	60	6	0.5	1	0.22	1	2	
Th	ppm	60	128	0.5	2	0.66	11	49	
La	ppm	60	1965	3	18	0.65	83	373	
Ce	ppm	60	2140	7	33	0.60	131	523	
Nd	ppm	60	654	2.5	12	0.49	36	109	
Sm	ppm	60	116.5	1.5	3.7	0.37	8.7	20.4	
Eu	ppm	60	31.4	0.25	1.2	0.39	2.9	7.1	
Tb	ppm	60	8.1	0.1	0.4	0.46	1.3	3.6	
Yb	ppm	60	5.7	0.6	1.8	0.15	2.6	3.7	
Lu	ppm	60	1.1	0.2	0.4	0.13	0.5	0.7	
La+Ce+Nd	ppm	60	3964	14	66	0.59	255	985	

Remarks : Standard deviation is shown in logarithmic scale.

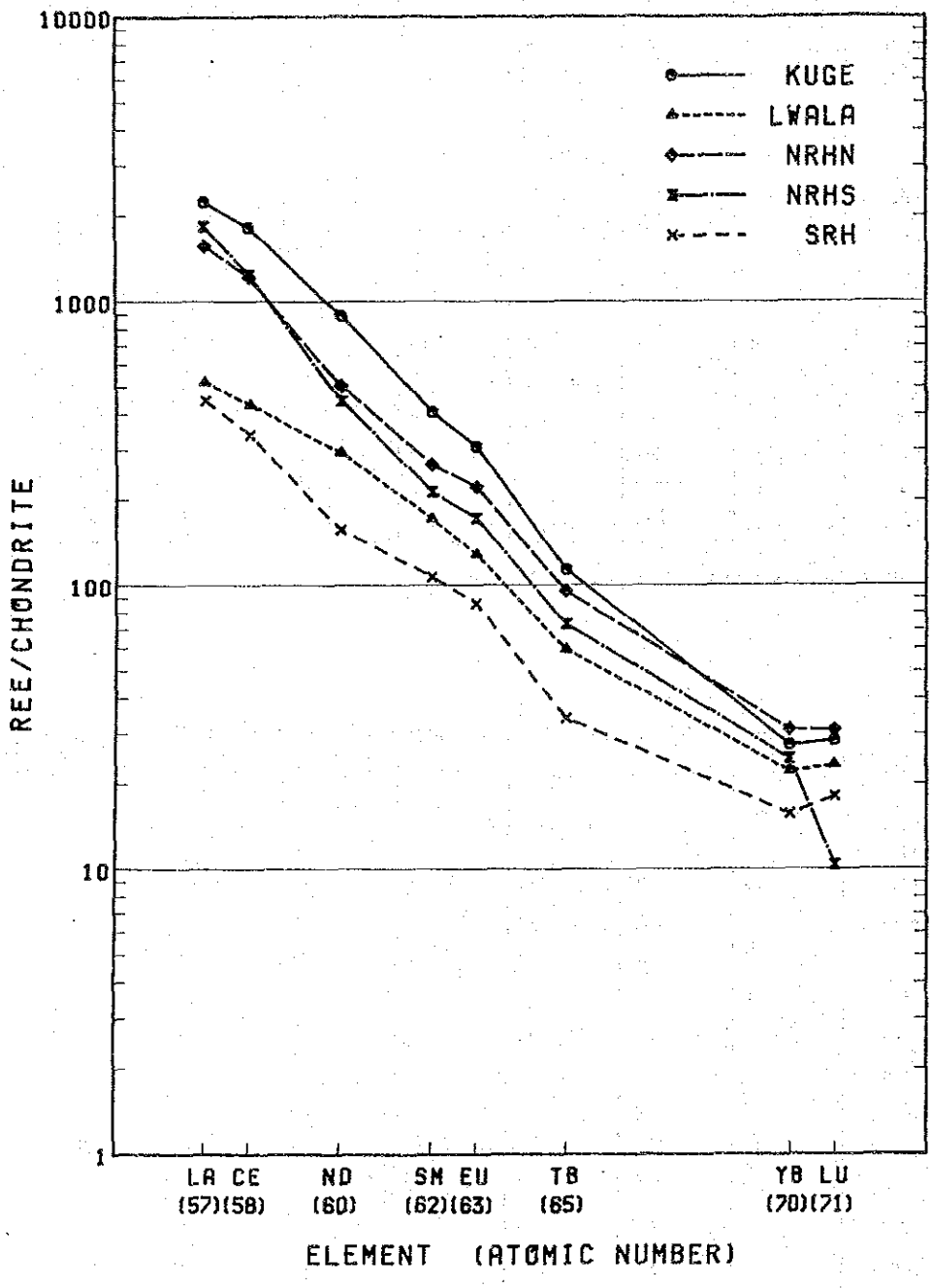

Fig. II – 3 – 1 Chondrite-Normalized REE Patterns by Survey Sector

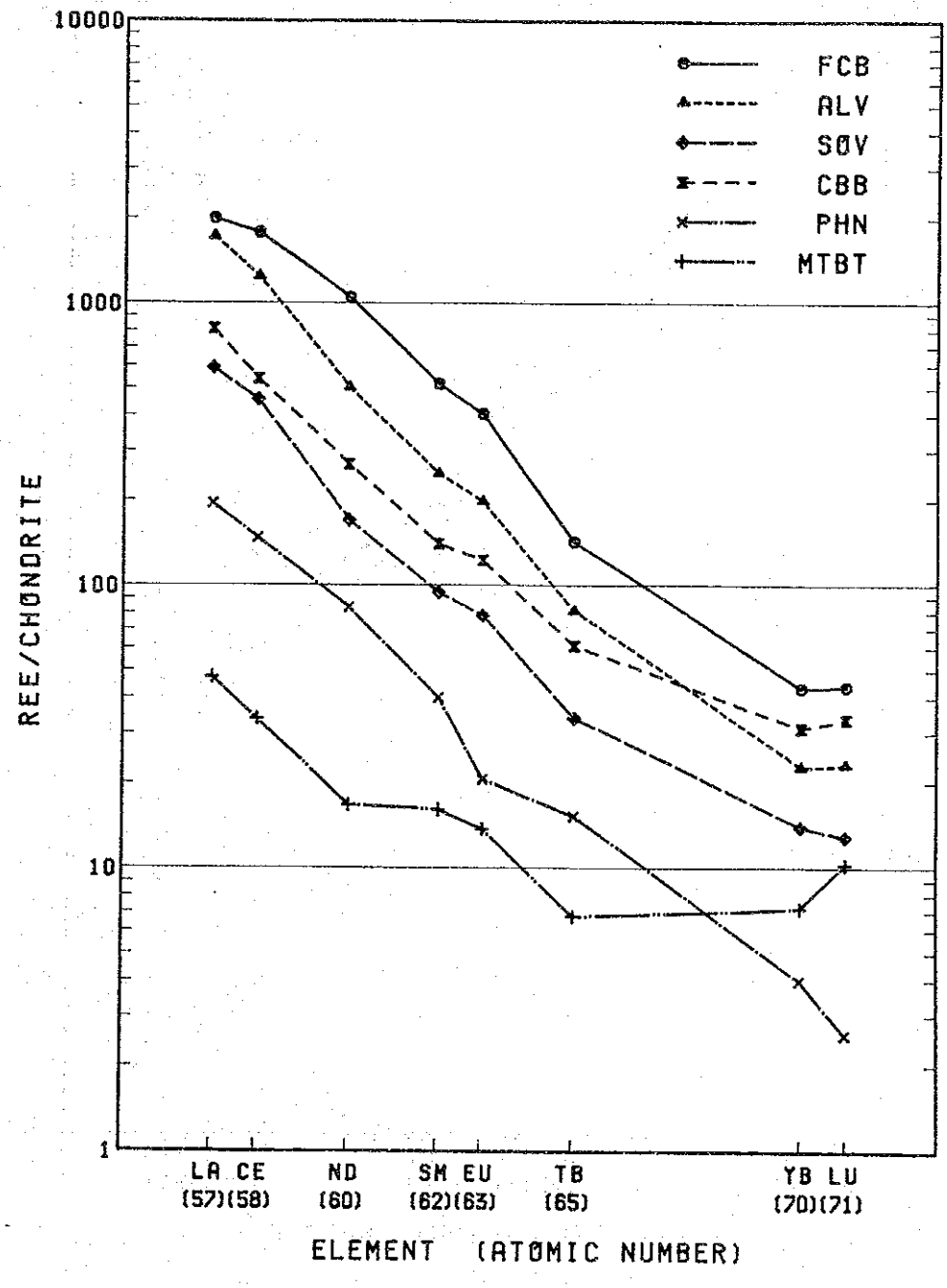

Fig. II – 3 – 2 Chondrite-Normalized REE Patterns by Rock Type in All Survey Sectors

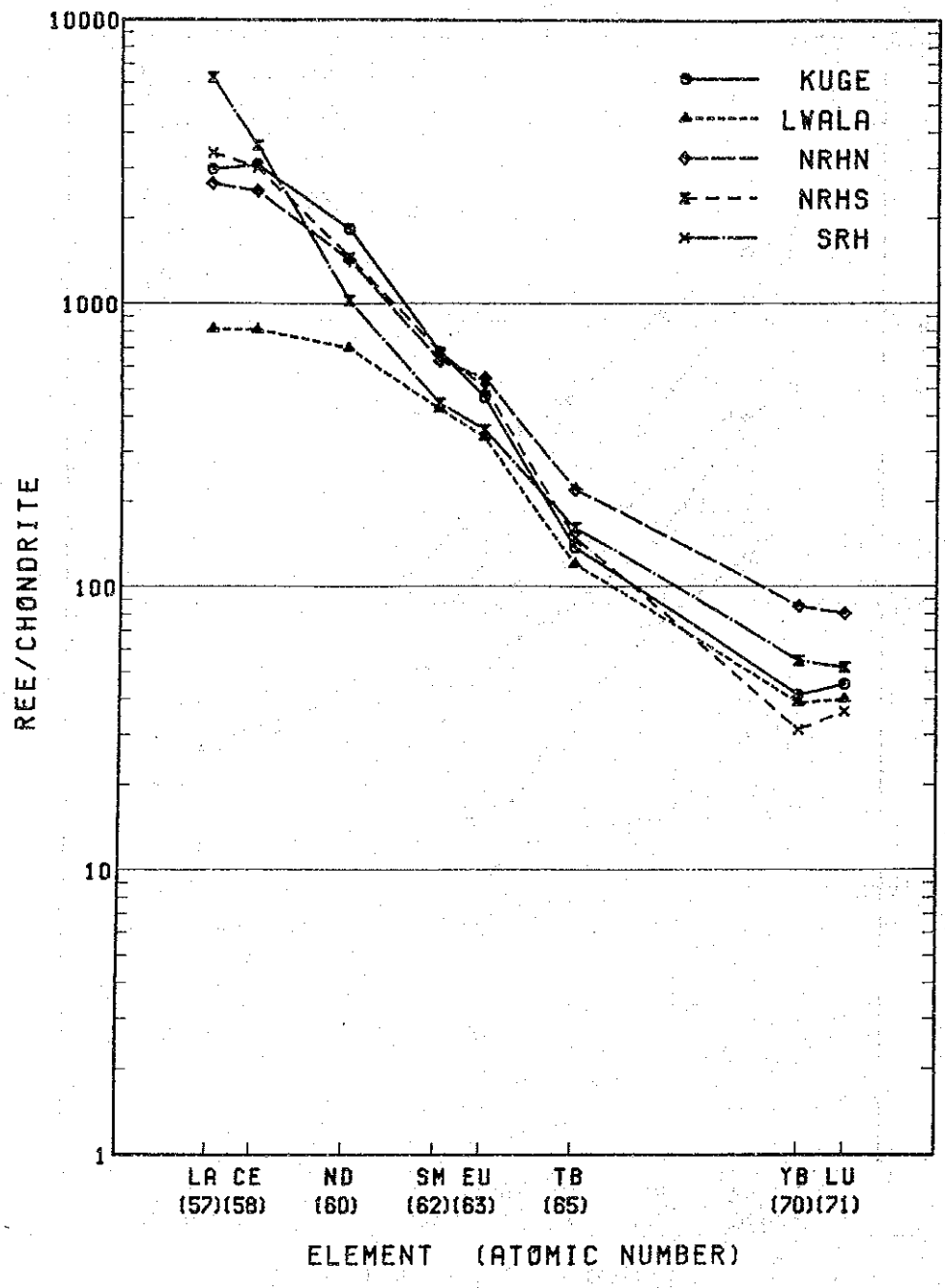

Fig. II – 3 – 3 Chondrite-Normalized REE Patterns of Ferrocarbonatite by Survey Sector

CHAPTER 4 BURU HILL AREA

4–1 Methods of Survey

4–1–1 Outline

The Buru Hill Area, occupies a rectangular-shaped zone of 0.96 square kilometre,was selected from the semi-detailed-survey area of 4 square kilometres, which was intially called as the Buru Hill Area on the stage of the first-year programme (Phase 1, Fig. II–4–1).

A detailed geological survey and a diamond-drill exploration work have been carried out in the area during the current survey programme, Phase 2. The detailed geological survey programme includes a Trenching Survey and a Pit Survey.

4–1–2 Detailed geological survey

The standard cartography for a geological mapping, scale of which was 1:2,000 and covered an area of 2.64 square kilometres, was made by using the existing air photographs of 1:40,000 scale approximately.

The traverse lines, which were due east-west and north-south, surveyed by using 50m-measure tapes and compasses and connect 17 drill hole mouths on about 120 metres grids, were allocated in the area. The traverses had a 4 kilometres extension in total. Geological mapping works of 1:2,000 scale along the traverses were carried out. In addition, the works above by means of pacings were also carried out in and out of the Buru Hill Area environs. The surveyed extensions were totalled to be of 19 kilometres long.

Trenching surveys were carried out along the outer hems of mineralized zones to elucide an extension of a mineralized rock mass. A trench has a 1 metre width in average and a 1 metre depth, 1.8 metres in maximum. The 10 trenches were exavated in the area totalling 320 metres extensions. The geological trench mapping inside of the trenches having of 1:100 scale were implemented (Apx 96–105).

Pit surveys were also carried out on the southern and eastern hill sides of the Buru Hill Area, where the surface is mostly covered by overburden, to examine the presence of mineralizations. Circular pits, having 1.5 metres diameter and 2.1 to 3.2 metres depth, were excavated at 5 locations. Geological logs inside of pits were represented on 1:20 scale delineations (Apx 106).

Geological maps and cross sections of 1:2,000 scale were delineated by the compilations of the geological showings of route-mappings, trench- and pit-surveys in connection with that of diamond drill cores.

4–1–3 Diamond drill operations

The 16 short-hole drills, having a 50 metre-depth each, and 1 deep-hole drill, having a 200 metre-depth, 17 holes with 1,000 metres depths in total, were operated.

Drill holes were allocated at on 120 metre-interval grids to establish a whole covering of the mineralized zones in the Buru Hill Area.

Detailed examinations of drill cores by unaided eye were carefully made to summarize the drill core logs. Necessary samples of minerals and rocks were collected to be sent to laboratory tests. Mineralized portions of the drill cores were chemically analysed at an every intersected portion to ores. The geological cross sections with drill hole logs projections were delineated after geological compilations of surface mappings and drill logs. The results of the chemical analyses of ores were applied to the estimations of inferred ore reserves and grades.

4–2 General Geology

4–2–1 Regional geology in the area

The Buru Hill Area is situated in the eastern region of the Kavirondo Rift, east-northeast to south-southwest or east-west directional, and traverses a basement rock area in western Kenya.

The Kavirondo Rift, regarded as one of the branch from the Kenya Rift Valley, is characterized by an alkaline rock occurrence represented by a carbonatite-alkaline plutonic rock activity and also a nepheline bearing volcanic rock activity.

The eastern province of the Kavirondo Rift occupies an extensive volcanic rock area of nephelinite-basalt, which is geologically successive to the Kenya Rift Valley. Tindred volcanic rock is situated in north-eastern portion of the Buru Hill Area, jointly with Kericho phonolite towards south.

The Tindred valcano is geologically characterized by having both volcanic activities of Rift Valley type and alkaline volcanic type of Kavirondo Rift and is associated with carbonatites in its parasite volcano, the Legetet Hill. The Buru Hill is located on a south-western extension of an alignment connecting the centre of Tindred volcano and Legeted Hill and is considered to be having a possible geological relation to the Tindred valcano.

The Buru Hill, intrudes into gneiss of a 100 square kilometres extent and has an area of 0.4 square kilometre, is observed as a small hill of jutting inlier in the vicinity of the geological boundary of Tindred and Kericho valcanos. Surroundings of the Buru Hill are mostly composed of granitoid gneiss and are geologically correlated to the Mozambique metamorphic rocks.

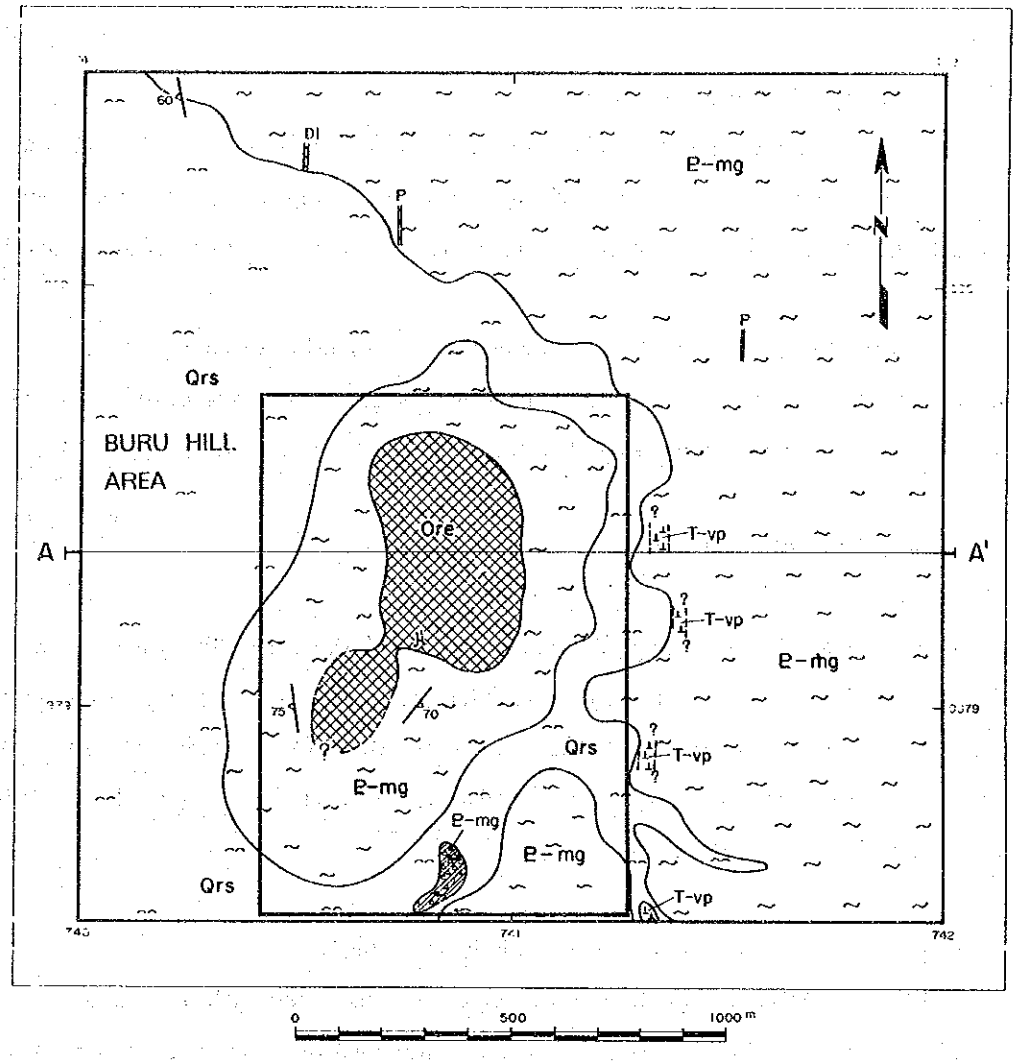

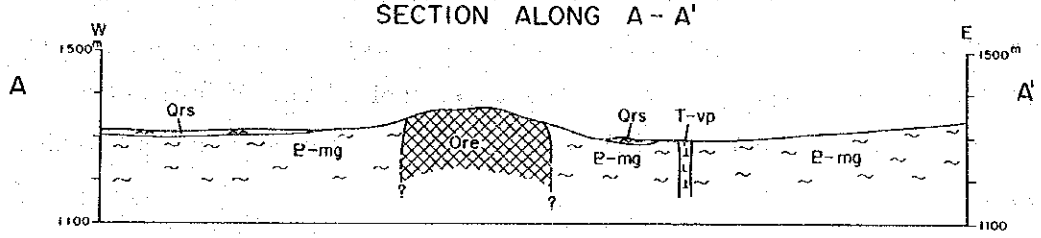

LEGEND

Qrs		Surficial deposits
T-vp		Phonolite
DI		Dolerite dyke
P		Pegmatite and segregation veins
Ore		"ORE" (vent agglomerate)
P-mg		Granitoid gneiss

Silicified and brecciated zone

Strike and dip of gneissosity

Portal of inclined shaft

A ——— A' Line of section

Fig. II – 4 – 1 Geological Map of the Buru Hill Area (Phase I Results)